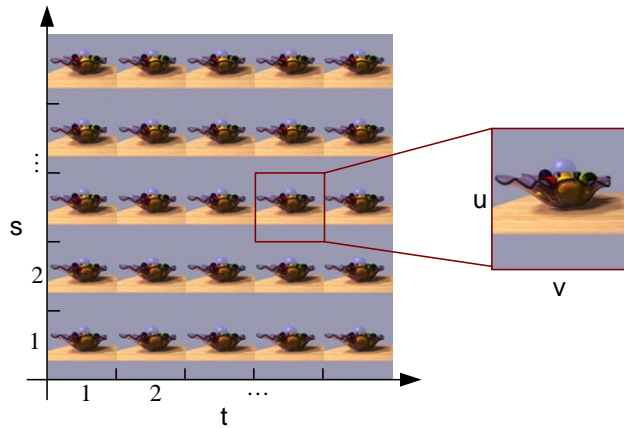Electrical *&* Computer
ENGINEERING

A Survey on Image-Based Rendering

- Representation, Sampling and Compression

Cha Zhang and Tsuhan Chen
Advanced Multimedia Processing Lab

Technical Report AMP 03-03
June 2003

Electrical and Computer Engineering
Carnegie Mellon University
Pittsburgh, PA 15213

Abstract

Image-based rendering (IBR) has attracted a lot of research interest recently. In this paper, we survey the various techniques developed for IBR, including representation, sampling and compression. The goal is to provide an overview of research for IBR in a complete and systematic manner. We observe that essentially all the IBR representations are derived from the plenoptic function, which is seven dimensional and difficult to handle. We classify various IBR representations into two categories based on how the plenoptic function is simplified, namely restraining the viewing space and introducing source descriptions. In the former category, we summarize six common assumptions that were often made in various approaches and discuss how the dimension of the plenoptic function can be reduced based on these assumptions. In the latter category, we further categorize the methods based on what kind of source description was introduced, such as scene geometry, texture map or reflection model. Sampling and compression are also discussed respectively for both categories.

I. Introduction

One might remember that in the movie *Matrix*, the scene with Keeanu Reeves dodging the bullets might be one of the most spectacular images ever caught on camera. This filming technology is what the movie producers called "Flo-Mo". "Flo-Mo" lets the filmmakers shoot scenes where the camera moves at a normal speed while the action is frozen or happens in slow motion. Two movie cameras and 120 computer-controlled still cameras were used in that scene. Similarly, the Eyevision system developed by CBS [11], which consisted of 33 cameras spaced approximately 6 degrees apart around the rim of the stadium, was used in a live broadcast of Super Bowl game in Jan. 2001. It provided a unique 3D view of selected plays in a 270-degree stop action image. These novel viewing experiences were brought to us by image-based rendering (IBR), which has been a very active research topic recently. By capturing a set of images or light rays in the space, the goal of IBR is to reproduce the scene correctly at an arbitrary viewpoint, with unknown or limited amount of geometry. Compared with geometric models that dominate the traditional 3D rendering pipelines, images are easier to obtain, simpler to handle and more realistic to render. Moreover, since image processing is one of the most widely studied research topics in the literature, IBR has attracted many researchers from different communities, including graphics, vision and signal processing.

Since the goal of IBR is to capture and render the 3D world, let us first see how the world can be described. One possible solution is to record all the objects in the world and their interactions, which we call a *source description*. The traditional model-based rendering approach adopts such a description: shapes of the objects are represented by certain geometric models; properties of the object surfaces are described by texture maps and reflection models; lighting and shading are the results of interaction between the light sources and objects, etc. The source description is often compact and insightful, because it tells how the world is composed. However, it has the disadvantage that such a description is not always available. From what we can observe with our eyes or cameras, deriving the source description is not trivial, and has been the goal of computer vision for more than twenty years with limited success.
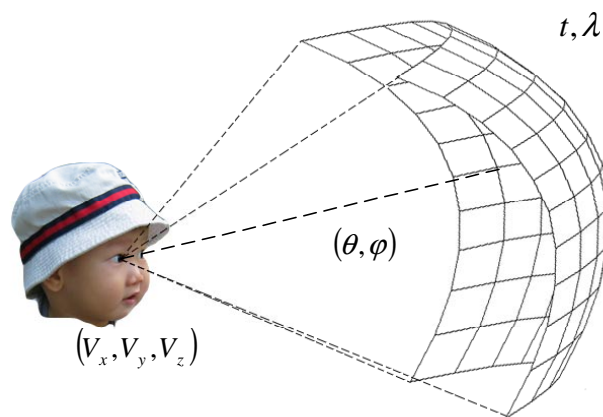

Figure 1 The 7D plenoptic function.

An alternative way to describe the world is through the *appearance description*. The appearance of the world can be thought of as the dense array of light rays filling the space, which can be observed by posing eyes or cameras in the space. These light rays can be represented through the *plenoptic function*, proposed by Adelson and Bergen [2]. As shown in Figure 1, the plenoptic function is a 7D function that models a 3D dynamic environment by recording the light rays at every space location (V_x, V_y, V_z), towards every possible direction (θ, φ), over any range of wavelengths (λ) and at any time (t), i.e.,

$$l^{(7)}(V_x, V_y, V_z, \theta, \varphi, \lambda, t) \tag{1}$$

As pointed out by Adelson and Bergen [2]:

> *The world is made of three-dimensional objects, but these objects do not communicate their properties directly to an observer. Rather, the objects fill the space around them with the pattern of light rays that constitutes the plenoptic function, and the observer takes samples*

from this function. The plenoptic function serves as the sole communication link between the physical objects and their corresponding retinal images. It is the intermediary between the world and the eye.

When we take an image for a scene with a pinhole camera[1], the light rays passing through the camera's center-of-projection are recorded. They can also be considered as samples of the plenoptic function. As image-based rendering is based on images, it adopts the appearance description. We define IBR under the plenoptic function framework as follows:

Definition - image based rendering*: Given a continuous plenoptic function that describes a scene, image-based rendering is a process of two stages – sampling and rendering[2]. In the sampling stage, samples are taken from the plenoptic function for representation and storage. In the rendering stage, the continuous plenoptic function is reconstructed with the captured samples.*

The above definition reminds us about what we typically do in signal processing: given a continuous signal, sample it and then reconstruct it. The uniqueness of IBR is that the plenoptic function is 7D – a dimension beyond most of the signals handled before. In fact, the 7D function is so general that, due to the tremendous amount of data required, no one has been able to sample the full function into one representation. Research on IBR is mostly about how to make reasonable assumptions to reduce the sample data size while keeping reasonable rendering quality.

There have been many IBR representations invented in the literature. They basically follow two major strategies in order to reduce the data size. First, one may restrain the viewing space of the viewers. Such constraints will effectively reduce the dimension of the plenoptic function, which makes sampling and rendering manageable. For example, if we limit the viewers' interest to static scenes, the time dimension in the plenoptic function can be simply dropped. Second, one may introduce some source descriptions into IBR, such as the scene geometry. Source description has the benefit that it can be very compact. A hybrid source-appearance description is definitely attractive for reducing the data size. To obtain the source description, manual work may be involved or we may resort to computer vision techniques.

---

[1] Throughout this paper, we assume that the cameras we use are pinhole cameras. Most of the IBR technologies in the literature made such assumption. The only exception, as far as the authors know, is the work by Isaksen *et al.* [47], where the effects of various aperture and focus were studied.

[2] We believe that considering IBR as a generic term for the techniques of both sampling and rendering is more appropriate than the conventional definition in [82]. In the sections that follow, *IBR rendering* will be used to refer to the rendering stage specifically.

Once the IBR representation of the scene has been determined, one may further reduce the data size through sampling and compression. The sampling analysis can tell us what is the minimum number of images / light rays that is necessary to render the scene at a satisfactory quality. Compression, on the other hand, can further remove the redundancy inside and between the captured images. Due to the high redundancy in many IBR representations, an efficient IBR compression algorithm can easily reduce the data size by tens or hundreds of times.

In this paper, we survey the various techniques developed for IBR. Although other classification methods are possible [48], we classify the techniques into two categories based on the strategies they follow. Section II presents IBR approaches that restrain the viewing space. Section III discusses about how to introduce source descriptions in order to reduce the data size. Sampling and compression are discussed for different IBR representations in different sections. Conclusions and future work are given in Section IV.

II.   Restraining the Viewing Space

If the viewing space can be constrained, the amount of images required for reproducing the scene can be largely reduced. Take an extreme example: if the viewer has to stay at one certain position and view along one certain direction, an image or a video sequence captured at that position and direction is good enough for representing the scene. Another example is branch movies [68][108][85], in which segments of movies corresponding to different spatial navigation paths are concatenated together at selected branch points, and the user is forced to move along the paths but allowed to switch to a different path at the branch points.

A. Commonly Used Assumptions to Restrain the Viewing Space

There is a common set of assumptions that people made for restraining the viewing space in IBR. Some of them are preferable, as they do not impact much on the viewers' experiences. Some others are more restrictive and used only when the storage size is a critical concern. We list them below roughly based on their restrictiveness.

Assumption 1: As we are taking images of the scene for IBR, we may simplify the wavelength dimension into three channels, i.e., the red, green and blue channels. Each channel represents the integration of the plenoptic function over a certain wavelength range. This simplification can be carried out throughout the capturing and rendering of IBR without noticeable effects. Almost all the practical representations of IBR make this assumption.

Assumption 2: The air is transparent and the radiances along a light ray through empty space remain constant. Under this assumption, we do not need to record the radiances of a light ray on

different positions along its path, as they are all the same. To see how we can make use of this assumption, let us limit our interest to the light rays leaving the convex hull of a bounded scene (if the viewer is constrained in a bounded free-space region, the discussion hereafter still applies). Under Assumption 2, the plenoptic function can be represented by its values along an arbitrary surface surrounding the scene. This reduces the dimension of the plenoptic function by one. The radiance of any light ray in the space can always be obtained by tracing it back to the selected surface. In other words, Assumption 2 allows us to capture a scene at some places and render it at somewhere else. This assumption is also widely used, such as in [62][37][119]. However, a real camera has finite resolution. A pixel in an image is in fact an average of the light rays from a certain area on the scene surface. If we put two cameras on a line and capture the light ray along it, they may have different results, as their observing area size on the scene surface may be very different. Such resolution sensitivity was pointed out by Buehler *et al.* in [10].

Assumption 3: The scene is static, thus the time dimension can be dropped. Although a dynamic scene includes much more information than a static one, there are practical concerns that restrict the popularity of dynamic IBR. One concern is the sample data size. We all know that if we capture a video for a scene instead of a single image, the amount of data may increase for about 2 or 3 orders of magnitude. It can be expected that dynamic IBR will have the same order of size increase from static IBR. Moreover, IBR often requires a large amount of capturing cameras. If we want to record a dynamic scene, all these cameras must be present and capturing video together. Unfortunately, today's practical systems cannot afford to have that many cameras. The known IBR camera array that has the largest number of cameras may be the Stanford light field video camera [137], which consists of 128 cameras. This is yet not enough for rendering high quality images. Capturing static scenes does not have the above problem, because we can always use the time axis to compensate for the lack of cameras. That is, images captured at different time and positions can be used together to render novel views.

Assumption 4: In stead o moving in the 3D space, the viewer is constrained to be on a surface, e.g., the ground plane. The plenoptic function can then reduce one dimension, as the viewer's space location becomes 2D. Although restricting the viewer on a surface seems unpleasing, Assumption 4 is acceptable for two reasons. First, the eyes of human beings are usually at a certain height-level for walk-through applications. Second, human beings are less sensitive to vertical parallax and lighting changes because their two eyes are spaced horizontally. Example scenes using concentric mosaics [119] showed that strong effects of 3D motion and lighting change could still be achieved under this assumption.

Assumption 5: The viewer moves along a certain path. That is, the viewer can move forward or backward along that path, but he / she cannot move off the path. Assumption 5 reduces two dimensions from the full plenoptic function. Branch movies [68][108][85] is an example that takes this assumption. This assumption is also reasonable for applications such as virtual touring, where the viewer follows a predefined path to view a large scene [52][89].

Assumption 6: The viewer has a fixed position. This is the most restrictive assumption, which reduces the dimension of the plenoptic function by three. No 3D effects can possibly be perceived under this assumption. Nevertheless, under this assumption the representations of IBR can be very compact and bear much similarity to regular images and videos. Capturing such representations is also straightforward. Thanks to these benefits, the QuickTime VR™ technology [20] based on Assumption 6 has become the most popular one among all the IBR approaches in practice.

There is one important thing to notice. That is, the dimension reduced by the above six assumptions may not be addable. In particular, Assumption 2 does not help further save dimension so long as one of the Assumption 4, 5 or 6 is made. This is because when the viewer's position has certain constraints, usually the sampled light ray space intersects each light ray only at a single point, which makes Assumption 2 not useful any more. In the next subsection, we will show a concrete example with concentric mosaics [119].

B. Various Representations and Their Rendering Process

By making the assumptions mentioned above, the 7D plenoptic function can be simplified to lower dimensional functions, from 6D to 2D. A quick summary of some popular representations is given in Table 1. We will explain these techniques in detail.

6D – The surface plenoptic function

The surface plenoptic function (SPF) was first introduced in [149]. It is simplified from the full 7D plenoptic function using Assumption 2. As we discussed, when radiance along a light ray through empty space remains constant, the plenoptic function can be represented by its values on any surface surrounding the scene. SPF chooses the surface as the scene surface itself. For regular scene surface with dimension 2, the SPF is 6D: position on the surface (2D), light ray direction (2D), time (1D) and wavelength (1D). Although it is difficult to apply SPF for capturing real scenes due to unknown scene geometry, SPF was used in [149] for analyzing the Fourier spectrum of IBR representations (see more details in Section II-C). The *surface light field* [86][139] could be considered as dimension-reduced version of SPF.

7

Table 1 IBR representations with various viewing space constraints.

Dimension	Example Representations	Assumptions
7D	Plenoptic function	No
6D	Surface plenoptic function	(2)
5D	Plenoptic modeling	(1, 3)
5D	Light field video	(1, 2)
4D	Light field / Lumigraph	(1, 2, 3)
3D	Concentric mosaics	(1, 2, 3, 4)
3D	Panoramic Video	(1, 6) or (1, 3, 5)
3D	Branch movies	(1, 3, 5)
3D	Video	(1, 6)
2D	Image mosaicing	(1, 3, 6)
2D	Image	(1, 3, 6)

Take anyone among Assumption 1, 3 and 4, we may also obtain a 6D representation of the scene. However, a 6D function is still too much for a practical IBR system to capture and render.

5D – Plenoptic modeling and light field video

By ignoring wavelength and time dimensions (Assumption 1 and 3), McMillan and Bishop [82] introduced plenoptic modeling, which is a 5D function:

$$l^{(5)}\left(V_x, V_y, V_z, \theta, \varphi\right) \tag{2}$$

They record a static scene by positioning cameras in the 3D viewing space, each on a tripod capable of continuous panning. At each position, a cylindrical projected image was composed from the captured images during the panning. This forms a 5D IBR representation: 3D for the camera position, 2D for the cylindrical image. To render a novel view from the 5D representation, the close-by cylindrical projected images are warped to the viewing position based on their epipolar relationship and some visibility tests.

The light field video [137][145] is another 5D representation based on Assumption 1 and 2. It is a straightforward extension of the 4D light field, which will be explained in detail later. Light field video captures dynamic scenes using a multi-camera array. Due to hardware constraints, the number of cameras in the array is very limited at the current stage (128 in [137] and 64 in [145]). Therefore, aliasing or ghosting effects are visible from the rendered videos.

From Table 1 it is clear that any IBR representation below 5D will make Assumption 1. The other assumptions are optional and can be chosen to generate new representations. For example,

if we constrain the viewer to be on a surface (Assumption 4), we get another 5D representation. Although no work has been reported to take such a representation, it is obviously feasible. What we need to do is to put many cameras on the viewer's surface and capture video sequences. During the rendering, since we did not make Assumption 2, the rendering position is also restricted on that surface.

4D – Light field / Lumigraph

The most well-known 4D IBR representations are the light field [62] and the Lumigraph [37]. They both ignored the wavelength and time dimensions and assumed that radiance does not change along a line in free space (Assumption 1, 2 and 3). However, parameterizing the space of oriented lines is still a tricky problem. The solutions they came out happened to be the same: light rays are recorded by their intersections with two planes. One of the planes is indexed with coordinate (u,v) and the other with coordinate (s,t), i.e.:
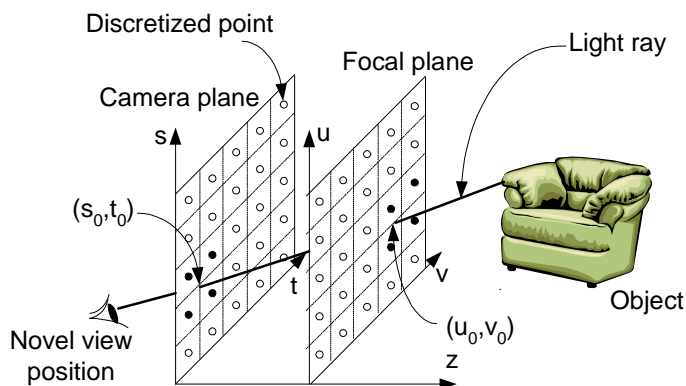
$$l^{(4)}(s,t,u,v) \tag{3}$$

Figure 2 One parameterization of the light field.

In Figure 2, we show an example where the two planes, namely the camera plane and the focal plane, are parallel. This is the most widely used setup. An example light ray is shown and indexed as (u_0, v_0, s_0, t_0). The two planes are then discretized so that a finite number of light rays are recorded. If we connect all the discretized points from the focal plane to one discretized point on the camera plane, we get an image (2D array of light rays). Therefore, the 4D representation is also a 2D image array, as is shown in Figure 3. To create a new view of the object, we just split the view into its light rays, which are then calculated by quad-linearly interpolating existing nearby light rays in the image array. For example, the light ray (u_0, v_0, s_0, t_0) in Figure 2 is interpolated from the 16 light rays connecting the solid discrete points on the two planes. The

new view is then generated by reassembling the split rays together. Such rendering can be done in real time [60][122] and is independent of the scene complexity.

We discuss briefly the difference between light field and Lumigraph. Light field assumes no knowledge about the scene geometry. As a result, the number of sample images required in light field for capturing a normal scene is huge [15][149]. To keep the amount of samples manageable, pre-filtering is applied during the capturing to reduce the light field signal's bandwidth [62]. On the other hand, Lumigraph reconstructs a rough geometry for the scene with an octree algorithm [37] to facilitate the rendering with a small amount of images (the geometry-image tradeoff is discussed later in Section III-B). Lumigraph also allows irregular sampling with a tracked hand-held camera. A hierarchical algorithm was proposed to resample the irregular samples onto the uniform grid on the camera and focal planes.
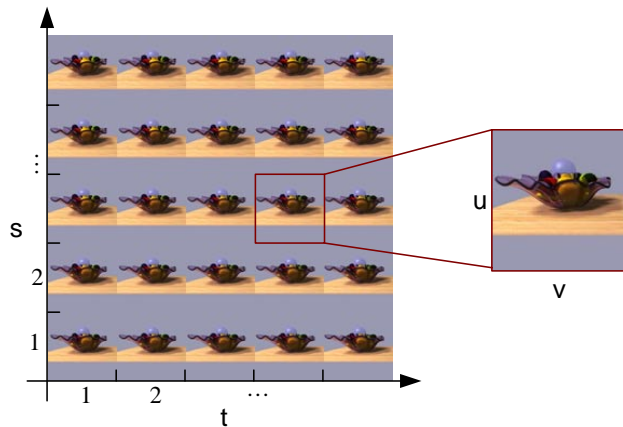

Figure 3 A sample light field image array: fruit plate.

As we mentioned before, when Assumption 2 is made, the plenoptic function can be represented by its values on an arbitrary surface surrounding the scene. Often, that surface is where we put our capturing cameras. Light field and Lumigraph both choose this surface to be a box – each face of the box is the camera plane of a two-plane parameterization above. In the spherical light field [45][14], a spherical surface was chosen for parameterization. Another interesting way to represent all the oriented lines in the space is the sphere-plane light field [14]. In this representation, a light ray is indexed by its direction (2D) and its crossing point (2D) with a plane perpendicular to its direction.

One thing to notice is that all the above representations are *structured* representations. There were some papers that tried to analyze such line space structures [62][13][41] and claimed that one is better than the other [13]. Nevertheless, all the above representations share one common drawback: they do not match with practical image capturing. For instance, in light field although

we may place cameras on the camera plane at the exact positions where discrete samples were taken, the pixel coordinates of the captured images cannot coincide with the focal plane samples. A sheared perspective projection was taken to compensate this [62]. In Lumigraph the images were taken with a hand-held camera so a resampling process was required any way. Spherical light field requires all the sample light rays passing through the corners of the subdivided sphere surface, which demands resampling for practical capturing. The sphere-plane light field does not have *pencil* (a set of rays passing through the same point in space [2]) in the representation so resampling is also needed. It would be attractive to store and render scenes from the captured images directly. In Section III-A we will discuss unstructured Lumigraph [10], which does not require the resampling.

Similar to the discussions in 5D, there are other possibilities to generate 4D IBR representations. For example, by making Assumption 1, 3 and 4, we may capture a static scene for a viewer to move smoothly on a surface [5][20]. If we make Assumption 1 and 5, we may record a dynamic event and allow a viewer to move back and forth along a predefined path.

3D – Concentric mosaics and panoramic video

Other than the assumptions made in light field (Assumption 1, 2 and 3), concentric mosaics [119] further restricts that both the cameras and the viewers are on a plane (Assumption 4), which "reduces" the dimension of the plenoptic function to three. In concentric mosaics, the scene is captured by mounting a camera at the end of a level beam, and shooting images at regular intervals as the beam rotates, as is shown in Figure 4. The light rays are then indexed by the camera position or the beam rotation angle α, and the pixel locations (u,v):

$$l^{(3)}(\alpha,u,v) \tag{4}$$

This parameterization is equivalent to having many slit cameras rotating around a common center and taking images along the tangent direction. Each slit camera captures a manifold mosaic, inside which the pixels can be indexed by (α,u), thus the name concentric mosaics. During the rendering, the viewer may move freely inside a rendering circle (Figure 4) with radius $R\sin(FOV/2)$, where R is the camera path radius and FOV is the field of view of the cameras. The rendering of concentric mosaics is slit-based. The novel view is split into vertical slits. For each slit, the neighboring slits in the captured images are located and used for interpolation. The rendered view is then reassembled using these interpolated slits.
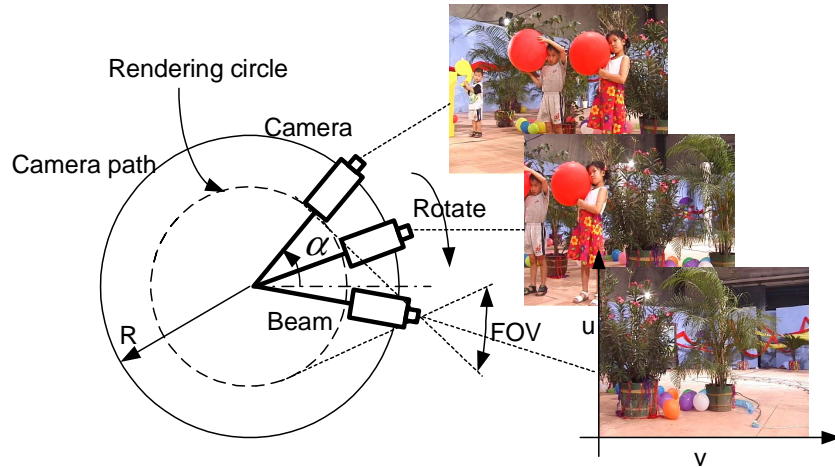
Figure 4 Concentric mosaic capturing.

There is a severe problem with concentric mosaics – the vertical distortion. Unfortunately, no matter how dense we capture the scene on the camera path, vertical distortion cannot be eliminated. In the original concentric mosaics paper [119], depth correction was used to reduce the distortion. That is, we need to have some rough knowledge about the scene geometry. Ignoring how difficult it is to obtain the geometry information, recall in the last subsection that the dimension reduced by Assumption 2 and Assumption 4 are not addable, we realize that the light ray space concentric mosaics is capturing is in fact still 4D. Recording it with 3D data must require extra information for rendering, in this case, the scene geometry.

Figure 5 Parallax observed from concentric mosaics rendered scenes.

Despite the severe vertical distortion, concentric mosaics is still a success. Capturing concentric mosaics is very simple. The viewer may experience significant horizontal parallax and lighting changes, as shown in Figure 5. A similar work to concentric mosaics is [50], where the camera path is a 1D straight line. Such scheme can be considered as a simplified version of light

field. On the other hand, concentric mosaics can be easily boosted to 4D if we align a vertical array of cameras at the end of the beam [65].

Another popular 3D IBR representation is the panoramic video [20][35][89]. It can be used for either dynamic (fixed viewpoint, Assumption 1 and 6) or static scenes (Assumption 1, 3 and 5). Compared with regular video sequences, the field of view in panoramic video is often 360°, which allows the viewer to pan and zoom interactively. If the scene is static, the viewer can also move around [20][52]. Capturing a panoramic video is an easy task. We simply capture a video sequence by a multi-camera system [35][123], or an omnidirectional camera [88], or a camera with fisheye lens [144]. Rendering of panoramic video only involves a warping from cylindrical or spherical projected images to planar projected images. Due to the convenience of capturing and rendering, the acceptable perceptual quality and the affordable storage requirement, multi-panorama representations are adopted for several systems used to capturing large-scale scenes, such as in [51][129]. Many commercial panoramic video systems are also available, such as iPIX immersive imaging from Internet Pictures Corp.[46], 360 One VR^{TM} from Kaidan [1], TotalView^{TM} from Be Here Technologies [132], Ladybug^{TM} from Point Grey [54], among many others.

2D – Image mosaicing

Image mosaicing composes one single mosaic with multiple input images. The output mosaic is a 2D plenoptic function. Often such mosaic is composed for increasing the field of view of the camera, with early applications in aerial photography [42][84] and cel animation [140]. Depending on the collection of the light rays recorded in the mosaic, image mosaicing techniques can be classified into two categories: single-center-of-projection mosaic or multiple-center-of-projection mosaic.

Figure 6 A 360° cylindrical panorama of the Confucious Temple, Shandong, China.

In most cases, the light rays recorded in the mosaic share the same center-of-projection (COP), which is called *panoramic mosaic* or *panorama* (Figure 6). The light rays are indexed by their directions, i.e.:

$$l^{(2)}(\theta, \varphi) \tag{5}$$

13

Although a panorama can be easily obtained by hardware intensive systems [83][88][144], the focus of research is on how to construct spherical or cylindrical panoramas by stitching multiple input images together [20][82][110][124]. Usually, the input images are taken from the same viewpoint and are related by 2D projective transforms. If the transforms are known in advance, images can be composed together easily [38]. Otherwise, a common technique is to establish at least four corresponding points across each image pair and find such transforms [39]. Other techniques for deriving these transforms without specific point correspondence have also been developed [124][125]. One practical issue is that the input images may not strictly share the same COP, which causes certain ghosting effects in the resultant mosaic. Such artifacts can be partially eliminated through local alignment algorithms [125][133].

In the more general scenario, the cameras of the input images can move in free form and the resultant mosaic has multiple COPs. In contrast to the panoramic mosaic where light rays are indexed by their directions, multiple-COP mosaic often indexes the light rays by a certain surface or manifold, thus it is also called *manifold mosaic*. The direction of the light rays is often perpendicular or tangential to the manifold surface. Recall in concentric mosaics [119] the 3D parameterization is equivalent to having many slit cameras rotating around a common center and taking images along the tangent direction. Each slit camera captures a manifold mosaic, which can be indexed by points on a 2D cylindrical surface ((α, u) as in Figure 4). All the light rays captured are tangential to that surface. In [99][100][157], manifold mosaic is constructed by stitching slit images together, assuming the motion of the camera is slow. Effectively, the surface that is used for light ray parameterization has various forms such as a plane, a cylindrical or other general surfaces. If center slits of the captured images are used for stitching, as was suggested in [100], the indexed light rays will be roughly perpendicular to these manifolds. A particularly interesting mosaic is constructed when the camera has forward or backward motion. Pipe projection was used to construct the mosaic on a pipe surface [101].

The rendering of image mosaicing is very simple. For panoramic mosaic, we often perform a warping from the cylindrical or spherical projected mosaic to planar projected images, as what we have done for panoramic video. Such a warping is often unknown in a general manifold mosaic. Therefore regions of the mosaic may be used directly for rendering, as long as the field of view of the rendered image is small enough [140]. Notice that in both cases, the motion of the viewer is very restricted. In a panoramic mosaic the viewer can only change his/her view direction, while in a manifold mosaic the viewer can only move along a fixed surface/path and towards a fixed direction. It is possible to alleviate the restraints by capturing multiple mosaics. The QuickTime

hopping [20] and the manifold hopping [121] are two such extensions for panoramic mosaic and manifold mosaic, respectively.

Other than increasing the field of view of the camera, image mosaicing can also be used to increase the image resolution, namely *super-resolution*. We refer the reader to [9] for a review of this area.

C. Sampling

In the last subsection, we discussed the various representations IBR may take and their rendering schemes, given that different viewing space constraints are employed. This answers the question *how to sample and reconstruct the plenoptic function*. However, there is one more question to ask: *how many samples do we need for anti-aliasing reconstruction*? We refer this problem as the IBR sampling problem and discuss its answers in this subsection.

IBR sampling is a very difficult problem, as the plenoptic function is such a high dimensional signal. Obviously, the sampling rate will be determined by the scene geometry, the texture on the scene surface, the reflection property of the scene surface, the motion of the scene objects, the specific IBR representation we take, the capturing and the rendering camera's resolution, etc. Over-sampling was widely adopted in the early stages, as no solution to the sampling problem was available. To reduce the huge amount of data recorded due to over-sampling, people used to resort to various compression schemes to save the storage space, which will be described in Subsection D. This situation was improved in the year 2000, when several pioneering papers were published on IBR sampling [66][15][17].

As was pointed out in [17], IBR sampling is essentially a multi-dimensional signal processing problem. Following the classic sampling theorem [96][31], one may first find the Fourier transform of the plenoptic function and then sample it according to its spectrum bandwidth. Nevertheless, although performing the Fourier transform of the 7D plenoptic function is possible in theory, in practice we have to reduce the dimension of the signal. Again we check the assumptions discussed in Subsection A and see how they may affect our sampling analysis.

Based on Assumption 1, the wavelength dimension can be ignored in most IBR applications. Thus sampling along the wavelength axis can also be ignored. Assumption 2 claims that the radiance of a light ray along its path remains constant in empty space. This means that along the light ray path, one sample is good enough for perfect reconstruction. In reality, although the resolution of real cameras is finite and Assumption 2 may not be strictly valid [10], the sampling along the light ray path is still less interesting because the variation of the radiance is often too slow. Assumption 3 said that if necessary, the time dimension could also be ignored. In practice,

even if we are capturing a dynamic scene, sampling on the time axis is often determined by the camera's frame rate and the property of the human eyes' temporal perception [23]. Due to the above reasons, most IBR sampling work in the literature [66][15][77][149] was for the light field and concentric mosaics.

The earliest IBR sampling work was by Lin and Shum [66]. They performed sampling analysis on both lightfield and concentric mosaics with the scale-space theory. The world is modeled by a single point sitting at a certain distance to the cameras. Assuming using constant depth and bilinear interpolation during the rendering, the bounds are derived from the aspect of geometry and based on the goal that no "spurious detail" should be generated during the rendering (referred as the causality requirement). Although the viewpoint of their analysis is rather interesting, this method is constrained by the simple world model they chose. The texture and the reflection model of the scene surface and occlusions are hard to analyze with such a method.

In [15], Chai *et al.* first proposed to perform the light field sampling analysis in the classic framework, i.e., applying Fourier transform to the light field signal, and then sampling it based on its spectrum. Assuming Lambertian surface and no occlusions, they found that the light rays represented by the plenoptic function have certain correspondence among themselves. For illustration purpose, we show a simplified 2D light field in Figure 7 (a). Notice that the camera plane and focal plane in Figure 2 degenerate to lines in 2D. A local discretization of the focal line was adopted in their analysis.

(a)   (b)

Figure 7 (a) The light ray correspondence in a 2D light field. (b) The spectrum of light field obtained in [15].

We may easily see the following relationship from Figure 7 (a):

$$l^{(2)}(t,v) = l^{(2)}\left(0, v - \frac{ft}{z(t,v)}\right)$$

(6)

where $z(t,v)$ is the scene depth of the light ray (t,v). When the scene is at constant depth $z(t,v) = z_0$, its Fourier transform can be written as:

$$L^{(2)}(\Omega_t, \Omega_v) = L'(\Omega_v)\delta\left(\frac{f}{z_0}\Omega_v + \Omega_t\right)$$ (7)

where $L'(\Omega_v)$ is the Fourier transform of $l^{(2)}(0,v)$ and $\delta(\cdot)$ is the 1D Dirac delta function. Obviously the spectrum has non-zero values only along a line. When the scene depth is varying between a certain range, a "truncating windows" analysis was given in the paper, which concludes that the spectral support of a lightfield signal is bounded by the minimum and maximum depths of objects in the scene only, no matter how complicated the scene is (Figure 7 (b)). Such analysis provides a fairly good first-order approximation of the spectrum analysis of IBR. However, the dependency on mapping images captured at arbitrary position to that at the origin prevents it from being applied to more complicated scenes such as non-Lambertian surface, scenes with occlusions and other IBR methods such as concentric mosaics.

Marchand-Maillet and Vetterli [77] performed Fourier analysis for scenes with functional surfaces. Instead of mapping all the images into one, they fixed the light ray direction and tried to find a one-to-one mapping from points on the scene surface to the camera plane. This one-to-one mapping is valid when no occlusion occurs. They showed that even when there is no occlusion, a band-limited signal pasted on a functional surface will not result in a band-limited lightfield spectrum.
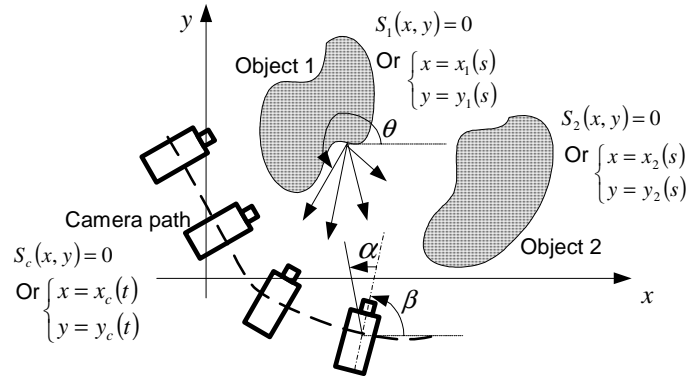

Figure 8 2D surface plenoptic function and general IBR capturing.

Noticing the fact that when Assumption 2 is made, the plenoptic function is equivalent to the surface plenoptic function (SPF), Zhang and Chen [149] proposed to consider the relationship between the SPF and the IBR representation for spectral analysis. Figure 8 shows a simple example of a 2D world. The SPF records the light rays emitted/reflected from the scene surface,

represented as $l_i^{(2)}(s,\theta)$, where s is the arc length on the scene surface curve; θ is the direction; i is the index of objects. The IBR representation can be written as $l_c^{(2)}(t,\alpha)$, where t is the arc length on the camera path, α is the light ray direction. There exists an *onto* mapping from $l_i^{(2)}(s,\theta)$ to $l_c^{(2)}(t,\alpha)$ due to the light ray correspondence. By assuming certain spectrum property of the SPF, the paper showed that it is possible to obtain the spectrum of the IBR representation, even when the scene is non-Lambertian or occluded. Moreover, the same methodology is applicable for concentric mosaics. "Truncating windows" analysis can also be used when the scene geometry is not available.

Same as in [77], analysis in [149] also showed that the spectrum of the IBR representation is very easy to be band-unlimited. However, from an engineering point of view, most of the signal's energy is still located in a bounded region. We may sample the signal rectangularly [15] or non-rectangularly [148] based on the high-dimensional generalized sampling theory [31]. Surprisingly, the non-rectangular sampling approach [148] does not show much improvement over the rectangular one considering the gain in rendering quality and the extra complexity introduced during the capturing and rendering.

It is also possible to sample the images non-uniformly for IBR [112][150][151]. Since most of these approaches were discussed assuming certain knowledge about the scene geometry, we discuss them in Section III-C.

D. Compression

Although we may reduce the number of images we take for IBR to the minimum through the sampling analysis, the amount of images needed is still huge. For instance, the example scenes in [15] shows that with constant depth rendering, the number of required images is on the order of thousands or tens of thousands for light field. To further reduce the storage requirement for IBR, data compression is the solution.

IBR compression bears much similarity as image or video compression, because IBR is often captured as a sequence of images. In fact, most of the IBR techniques developed so far are originated from image or video compression. On the other hand, IBR compression has its own characteristics. As pointed out in [64], images in IBR have better cross-frame correlations because of the regular camera motions. Thus we should expect better compression performance for IBR. The reaction of the human visual system (HVS) to the distortions introduced in IBR compression is also worth studying at very high compression ratio. Most importantly, since during the IBR rendering any captured light ray may be used for interpolation, it is desirable that

the compressed bitstream is random-accessible so that we do not need to decompress all the light rays into memory. Such property is also important for online streaming of IBR data.

Vector quantization (VQ) is often the first resort for data reduction in IBR [62][119]. As a universal method, vector quantization provides reasonable compression ratio (around 10:1 to 20:1 as reported) and fast decoding speed. The code index of VQ is fixed-length, which is random-accessible and has potential applications in robust online streaming. On the other hand, VQ does not fully make use of the high correlations inside and between the captured images, thus the compression ratio is not satisfactory.

The various image compression algorithms can also be applied to individual IBR images without change. Miller *et al.* used the standard DCT-based JPEG algorithms for light field compression [86] and obtained a compression ratio higher than that of VQ (around 20:1). The more recent wavelet-based JPEG2000 standard [127] may further improve the performance, as well as add features such as scalability. Since variable length coding (VLC) is employed, the light ray access speed is not as fast as VQ. Yet it is still good enough for real-time rendering. The limitation is that the inter frame correlation is not utilized, thus the compression ratio is still relatively low.

Most of the IBR compression methods proposed so far [75][153][61][72][71] resemble video coding, with certain modifications to the specific characteristics of IBR data. To see the close relationship between them, we list the techniques in video coding and IBR compression in parallel in Table 2. Detailed explanation follows.

The basic video coding techniques include motion compensation (MC), discrete cosine transform (DCT), quantization and VLC, among many others. The images are divided into two categories: intra frames and inter frames. Intra frames are often distributed uniformly and encoded independently, while inter frames are predicted from neighboring intra frames through MC. The early and widely adopted video coding standard, MPEG-2 [87], is a good example for all these techniques. An intuitive approach for IBR compression is to apply these methods directly for the IBR image sequence. In [120], Shum et al. proposed to compress the concentric mosaics with MPEG-2. Both the captured images and the rebinned manifold mosaics were used as frames in MPEG-2. The compression ratio was about 50:1. To facilitate random access, pointers to the start positions of each vertical group of macroblocks (MB) were built into the bitstream. Direct extension of the above approach for panoramic video and simplified dynamic light field (videos taken at regularly spaced locations along a line) were given in [91] and [16], respectively.

Table 2 Comparison between video coding and IBR compression techniques.

Video Coding Techniques	IBR Compression Extensions	IBR Compression References
Motion compensation (MC), DCT, quantization, VLC, etc	Constrained MC structure, indexed bitstream	[120][91][16]
MC tools such as global MC, multiple-frame MC, etc.	MC specific for IBR	[153] [73][74][152][131]
Sprite coding	-*	[61]
Model-based MC	Model-aided MC	[72][76]
Scalable video coding	-	[90][131][74]
Arbitrary shaped video object coding	-	[19]
3D wavelet coding	3D and 4D wavelet coding	[71][142][143] [103][76][36][55]
Error resilient coding, joint-source-channel coding, online streaming	-	[154][40][106]

* Here "-"means that the corresponding video coding technique can apply directly for IBR compression.
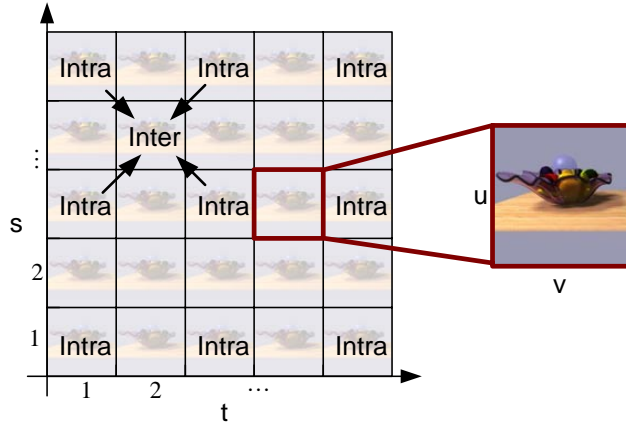
Figure 9 The 2D motion compensation structure for light field.

As the motion of the cameras during the IBR capturing is very regular, it is natural to replace the general MC module in MPEG-2 with more advanced methods for IBR compression. In [153], Zhang and Li proposed the reference block coder (RBC). RBC employs a two-stage MC scheme. The horizontal panning between neighboring captured images was first extracted as a global

horizontal translation motion vector. Local MC refinement was used to further reduce the MC residue. Another strength of RBC was the extensive usage of caches during the rendering, which guaranteed the so-called *just-in-time rendering*. In the light field, cameras are arranged on a 2D plane. Thus the MC structure should also be 2D. As shown in Figure 9, intra frames are uniformly distributed on the 2D plane. Given any inter frame, four neighboring intra frames are often available and can all be use for MC [73][75][152]. Hierarchical MC was proposed in [131][74][75], where images are grouped into different levels through down-sampling on the camera plane. The images at the lowest level are intra-coded. Higher level images are predicted from lower level images. Such hierarchical MC structure improves the compression ratio, but its bitstream may not be random accessible.

Further development on motion compensation includes sprite based coding and model based coding. In [61], Leung and Chen proposed a sprite based compression method for concentric mosaics. A sprite is generated by sticking the central slits of all the captured images. In fact, the result is roughly a cylindrical panorama. The sprite is intra coded and all the captured images are coded based on predictions from the sprite. Such a scheme has good random accessibility, and its compression ratio is comparable to that of [153]. When the scene geometry is available [32][107][114], it can greatly enhance the image prediction [72][76]. A hierarchical prediction structure is still adopted [72], where the intra coded images and the geometry model are used jointly to predict inter frames. In [76], images are mapped back onto the geometry model as view dependent texture maps. These texture maps are then encoded through a 4D wavelet codec. Model based IBR compression methods often report very high compression ratio, though such performance heavily relies on how good the geometry model is.

Two key components in the recent MPEG-4 video coding standard are the scalable video coding and arbitrary shaped video object coding [102]. Scalable video coding includes spatial scalability, temporal scalability, SNR fine granularity scalability (FGS), and object-based scalability. Ng et al. proposed a spatial scalability approach for the compression of concentric mosaics in [90]. By using a nonlinear perfect reconstruction filter bank, images are decomposed into different frequency bands and encoded separately with the MPEG-2 standard method. Consider the scenario of online streaming. A low-resolution image may be rendered first when the compressed base band bitstream arrives and refined later when more data are received. Temporal scalability is applicable to dynamic scene IBR representations such as light field video or panoramic video. Or, it can be considered as the scalability across different captured images. The above-mentioned hierarchical MC based IBR compression algorithms [131][74][75] are good examples. SNR FGS scalability and object-based scalability have not been employed in IBR

compression yet, but such methods should not be difficult to develop. Arbitrary shaped video object coding may improve the compression performance because it improves the motion compensation, removes the background, and avoids coding the discontinuity around the object boundary. It was adopted in a recent paper for light field compression [19].

3D wavelet coding presents another category of methods for video coding [128][93][130]. In [71], Luo *et al.* applied 3D wavelet coding for concentric mosaics. Nevertheless, its compression ratio is not satisfactory due the poor cross-frame filtering performance, which is consistent with the results reported in 3D wavelet video coding. A smart-rebinning approach was proposed in [143] which reorganized the concentric mosaics data into a set of panoramas. Such rebinning process greatly enhanced the cross-frame correlation and helped achieve very high compression ratio (doubled or even quadrupled that of RBC). A progressive inverse wavelet synthesis (PIWS) algorithm [142] was also proposed for fast rendering. Wavelet coding was further extended to 4D for light field compression, such as the work in [103][76][36][55].

Streaming the video bitstream over wired or wireless network has been a very attractive research topic recently. Many new techniques have been developed, such as error resilient coding, rate shaping, joint-source-channel coding, etc. Streaming IBR compressed data is also a very interesting topic, as it enables a user to walk through a realistic virtual environment. However, there are certain differences between video streaming and IBR streaming. For example, a frame in video is often associated with a critical time instance such as its playout deadline. Such deadline is not that critical in IBR streaming. Transmitted video is played back frame-by-frame, while in IBR the user may move freely as he/she wants and the light rays required by the current view are often distributed across multiple images. This brings some difficulty in distortion estimation [106]. In [154], the RBC compressed bitstream is transmitted over the Internet through a virtual media (Vmedia) access protocol. Only the bitstream associated with the current view is sent from the server to the client. The TCP/IP or UDP protocol is used and retransmission is requested if a packet is lost. Streaming high-resolution panoramic images with MPEG-4 was discussed in [40]. Recently a rate-distortion optimized streaming framework for light field transmission was proposed in [106]. Perfect advanced knowledge about the user's view trajectory is assumed. Significant gain was shown with this framework over heuristic packet scheduling. On the other hand, if the user's motion is unknown, prefetching [98] based on the user's historical motion may be a worth topic to study for IBR streaming.

III. Introducing Source Descriptions

Another strategy to make the image-based rendering data manageable is to introduce some source descriptions. Such descriptions can be the scene geometry, the texture map, the surface reflection model, etc. These descriptions can tell the correspondence between light rays, thus reduce the overall number of necessary light rays to be captured.

A. IBR with Various Source Descriptions

The major source descriptions employed in IBR are the scene geometry, the texture map and the surface reflection model. Among them the scene geometry is the most widely used. Texture map and reflection model are often used as additional descriptions on top of the scene geometry. A quick summary of the different approaches is given in Table 3.

Table 3 A quick summary of various approaches that introduce source descriptions.

Source Description		Reference
Scene geometry	Correspondence between images	View interpolation [21], view morphing [117], reference views [56], tensor space [6], etc.
	Dense (per pixel) depth map	LDI [117], LDI tree [18], MCOP [105], etc.
	Mesh or volumetric model	Unstructured Lumigraph [10], spatial-temporal view interpolation [134], view dependent geometry [104], etc.
Texture map (+ Scene geometry)		View dependent texture map [27], image-based visual hull [79], etc.
Reflection model (+ scene geometry)		Reflection space IBR [12], surface light field [139], etc.

1. Scene geometry

Given the scene geometry, light rays from the same surface point can be identified. Since most scene surfaces are close to Lambertian, or at least locally color consistent (light rays from the same surface point share the same color if their reflection directions are similar) [147], geometry can save the number of light rays to be captured for a scene [15]. In fact, as was pointed out by many researchers, there is a geometry-image continuum in the representations of scenes [49][59]. The more we know about the scene geometry, the smaller the amount of images we need for good rendering.

The scene geometry can be described in different forms, such as correspondence between images (e.g., optical flow), dense depth map, volumetric or mesh model, etc. In this subsection we classify the various approaches based on different geometry forms they take and present them one by one.

Correspondence between images

Any scene geometry information can be considered as knowledge about the correspondence between images. Here we specifically mean approaches that do not have an explicit geometry representation. Examples of such knowledge are point feature correspondences, disparity map, optical flow, etc. The idea is to find corresponding light rays in the captured image set for those in the novel view. In the photogrammetric community, such approaches are developed under the name of *transfer* methods.

Early work on this track was under the study of image morphing [7] and often involves certain manual help. For example, an animator needs to specify a set of feature correspondences, which form a control mesh. In [138], the novel view is generated by warping the control mesh through spline interpolation. A two-dimensional free-form deformation and Bézier Clipping was used to fulfill the same task in [92]. In [7], Beier and Neely defined a global transform/warping between the two images based on a set of matched line segments. For any view in between, the matched line segments in the novel view are first interpolated, which then determines the transform from one of the reference views to the novel view. A deformable surface model based morphing strategy that does not require the control mesh structure was also discussed in [58]. Recently, a feature-based light field morphing algorithm was proposed in [155].

View interpolation [21], proposed by Chen and Williams, eliminates the need of the human animator. Instead, the optical flow between the two images is assumed as known. To generate an in-between view of the input image pair, the offset vectors in the optical flow are linearly interpolated and the pixels in the source images are moved by the interpolated vector to their destinations in the novel view. View interpolation performs very well if the two input images are close to each other, so that visibility ambiguity is not an issue. On the other hand, the interpolated views will be physically exact only if the camera motion is perpendicular to the camera viewing axis. In [135] a mathematical formulation was given to show the conditions when linear interpolation is physically correct.

In [116][117], Seitz and Dyer proposed view morphing. View morphing guarantees that the rendered view is physically valid by introducing a prewarping stage and a postwarping stage. During the prewarping, the two reference images are rectified [44]. After the rectification, the two images share the same image plane and their motion becomes perpendicular to their viewing axis.

Linear interpolation is then used to get the intermediate view, followed by postwarping to compensate the rectification effect on that view.

The novel view in view interpolation and view morphing are often in between the two reference images. Laveau and Faugeras [56] first proposed to make use of the epipolar constraints [44], which enabled extrapolation. The novel view is generated from a set of weakly or fully calibrated reference views. The viewpoint and the retinal plane of the novel view are specified by manually selected four corresponding points. A dense disparity map is also assumed to be available. To render the novel view, a ray-tracing like algorithm is implemented, which for each rendered light ray find the corresponding light rays in the reference views through the epipolar constraint and the disparity map. Notice that when the reference views are weakly calibrated, only projective structure can be recovered [44], thus the resultant novel view may appear warped. Knowing the intrinsic parameters of the cameras (full calibration) will solve such problem.

In plenoptic modeling [82], a similar approach was proposed. The difference is that the reference view positions are known, and the reference views are now cylindrically projected panoramic views. Therefore, cylindrical epipolar constraints and dense angular disparity maps were used for novel view interpolation.
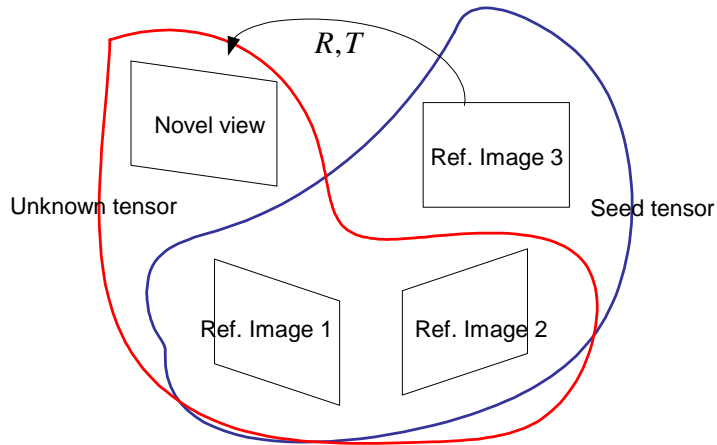

Figure 10 Obtain the tensor between a novel view and the two reference views from a seed tensor [6].

The epipolar constraint is between two images. For three images, there is another constraint represented by the trifocal tensor [44]. Given two views in correspondence and a tensor, the corresponding third view can be generated by a warping function. Avidan and Shashua proposed a view synthesis algorithm based on the above principle [6]. The key of their approach is the way to specify the tensor between two reference views and a novel view. As illustrated in Figure 10, given a seed tensor between the two reference views and an additional reference view (which could be a duplication of one of the two reference views), the unknown tensor could be obtained

25

by knowing the rotation and translation between the third reference view and the novel view. Therefore specification of a novel view is more direct compared with the epipolar constraint based methods such as [56], where manual selection of matching points is needed. Moreover, trifocal tensor based method is often more stable than the epipolar constraint based ones under certain singular camera configurations (e.g., when the camera centers are collinear).

In a recent approach Lhuillier and Quan [63] presented an interpolation algorithm based on joint view triangulation. Starting from some points of interest selected automatically, they first grow the matching points to their neighborhoods. Planar patches are then fit locally for regularization or removing outliers assuming the matching is piecewise smooth. The two reference views are then triangulated jointly. Novel views are interpolated by warping the matched triangles. A walk-through system based on a similar framework was also developed in [3].

Dense depth map

Another popular scene geometry representation is the dense depth map. It indicates the per-pixel depth values of the reference views. Such a depth map is easily available for synthetic scenes, and can be obtained for real scenes via a range finder.
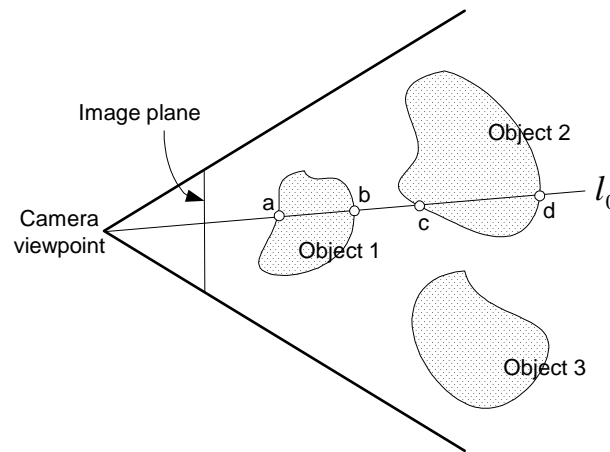

Figure 11 The layered depth image.

The simplest IBR representation with a dense depth map is a set of images and their depth maps [81][113]. An extension to the multiple-center-of-projection (MCOP) mosaic (Section II-B) was given in [105], where again a depth value is attached to each pixel in the MCOP image. In [118], Shade *et al.* proposed the sprite with depth and the layered depth image (LDI). Sprite with depth keeps an out-of-plane displacement component at each pixel in the sprite, which resembles the above-mentioned representations. LDI is a view of the scene from a single input camera view,

but with multiple pixels along each line of sight. Correspondingly, the depth map is also multi-valued for each pixel. This is shown in Figure 11. On the path of the light ray l_0, the depth and color value of point a, b, c and d are all recorded. Extensions to the LDI include the layered depth cube [69] and the LDI tree [18].

The rendering algorithms of IBR representations with dense depth map are often similar to each other. In [81], a 3D warping algorithm was proposed to render novel views that are close to a reference view. The pixels of the reference view are first projected back to their 3D locations and then re-projected to the novel view. To speed up the above process, Oliveira and Bishop [95] proposed to factorize the warping process into a simple pre-warping stage followed by a standard texture mapping. The pre-warp handles only the parallax effects resulting from the depth map and the direction of view. The subsequent texture-mapping operation handles the scaling, rotation, and remaining perspective transformation, which can be accelerated by standard graphics hardware. A similar factoring algorithm was performed for the LDI [118], where the depth map is first warped to the output image with visibility check, and colors are pasted afterwards.

One major problem in the above rendering methods is that holes may occur in the rendered view due to undersampling or disocclusion (scene is occluded in the reference view but visible in the novel view). By introducing multiple depth values along a light ray, the disocclusion problem is partially solved in the LDI representation [118]. In [113], because multiple images are available for rendering, holes due to disocclusion are also not serious as long as the number of images is large enough. The undersampling problem can also be solved by taking more images. The LDI tree [18] is a modified LDI approach which combines multiple reference views in to a single hierarchical representation, which maintains the resolution of each reference view in the data structure. On the other hand, even if holes do happen, they may be removed through algorithms such as splatting [78][118] or meshing [78][105].

Mesh or volumetric model

Mesh model is the most widely used components in model-based rendering. Despite the difficulty to obtain such a model, if it is available in image-based rendering, we should make use of it to improve the rendering quality.

Buchler *et al.* proposed the unstructured Lumigraph rendering [10], which addressed the above rendering problem. They first proposed eight goals for IBR rendering: use of geometric proxies; unstructured input; epipole consistency; minimal angular deviation; continuity; resolution sensitivity; equivalent ray consistency and real-time. These goals served as the guidelines of their proposed unstructured Lumigraph rendering approach. Weighted light ray interpolation was used to obtain light rays in the novel view. The weights are largely determined

by how good the reference light ray is to the interpolated one according to the goals. A clever weight blending field for the reference views is described to guarantee real-time rendering.

For real-world scenes, the geometry model we reconstruct is often in a volumetric form [37][134][115][32]. Although the volumetric model can be easily converted to a mesh model [70], sometimes it may be preferable to render with the volumetric model directly. The algorithm in [10] can be applied straightforwardly without any change. One concern about the volumetric model is that it has a finite resolution. To remove the granular effects in the rendered image due to finite resolution, in [134] a model smoothing algorithm was applied during the rendering, which greatly improved the resultant image quality.

Rademacher proposed an interesting approach called view dependent geometry [104]. Namely, the geometry used during the rendering may vary when the view position changes. Such approach is attractive for scenes where the geometry reconstruction algorithm can only obtain a model that is locally applicable, such as those obtained through stereo methods [111].

Image-based modeling

Scene geometry can often greatly improve the rendering quality, but acquiring the geometry is not a trivial task unless the scene is synthetic or a range finder is on hand. When no geometry is directly available, we may resort to computer vision techniques to reconstruct the scene geometry based on the captured images. Such techniques are called *image-based modeling*. Due to the close coupling of image-based rendering and image-based modeling, we see a clear convergence of the graphics community and the vision community [59].

As a survey of the various image-based modeling techniques is out of the scope of this paper, we refer the reader to the survey paper by Zhang [156] and by Oliveira [94] for more information.

2. Texture map (+ scene geometry)

Texture map is one of the most widely used source descriptions in model-based rendering. As texture maps are often obtained from real objects, a geometric model with texture mapping can produce very realistic scenes.

In image based rendering, when the scene geometry is available, it is possible to generate texture maps from the reference views. This has already been demonstrated in the 3D warping algorithm [81] for IBR representations with dense depth map mentioned before. Notice that in IBR we do not apply reflection models of the scene surface as we do in model-based rendering. A scene becomes Lambertian if both the geometry and the texture map are fixed. Such scenes may not be highly interesting. It is therefore natural to introduce texture maps that vary when the viewpoint changes, namely view dependent texture mapping (VDTM) [27].

In [27], Debevec *et al.* proposed to project the reference views onto the geometric model to form the texture map through a weighting scheme. The weights are determined by the angular deviation from the reference views to the virtual view to be rendered. Later a more efficient implementation of VDTM was proposed in [29], where the per-pixel weight calculation was replaced by a per-polygon search in a pre-computed lookup table. Note that VDTM is in fact a special case of the later proposed unstructured Lumigraph rendering [10].

The image-based visual hull (IBVH) algorithm [79] can be considered as another example of VDTM. In IBVH, the scene geometry was reconstructed through an image space visual hull [57] algorithm. A texture pixel was generated from the reference views by back projection using only the light ray with the smallest angular deviation. Such adaptation is partially due to the fact that only four cameras were used in IBVH.

3. Reflection models (+ scene geometry)

Other than the texture map, the appearance of an object is also determined by the interaction of the light sources in the environment and the surface reflection model. This becomes more obvious if the texture map is very simple (e.g., uniform color) and the object is highly specular, such as a simple mirror ball.

In image-based rendering, we often do not try to figure out what the scene object's reflection model is. Instead, we capture light rays that are reflected from the scene surface. Recall that such parameterization has been discussed under the name *surface plenoptic function* [149] in Section II-B. The advantages of recording only the reflected light rays are numerous: we do not need to derive the underlying surface reflection model any more; we do not need to model the complex light sources in a real environment; and we do not need to calculate the interaction between the light source and the reflection model. The downside is that the light source and the reflection model are now tightly coupled. Efforts need to be made for relighting the scene under different lighting conditions [141][26].

In [12], Cabral et al. proposed reflection space image-based rendering. Reflection space IBR records the total reflected radiance for each possible surface direction. Note the difference between such a radiance environment map and the traditional environment map, where the incoming radiance is stored [8][39]. The proposed radiance environment map is viewpoint dependent, thus a set of such maps are pre-computed before rendering, as the multiple images we often have in normal IBR representations. During the rendering, the radiance environment map is first interpolated/warped to the desired viewpoint and then used for novel view generation. An interesting application of radiance environment map is given in [25], where synthetic objects are rendered into real scenes. A probing mirror ball is used to obtain the radiance environment map at

the position the synthetic objects are located. A differential rendering technique allows for good results to be obtained when only an estimate of the local scene reflectance properties is known.

The above method assumes that if two surface points share the same surface direction, they have the same reflection pattern. This might not be true due to multiple reasons such as inter-reflections. A more general approach is to really capture the scene reflections at arbitrary surface points as in the surface plenoptic function [149]. By ignoring the time and the wavelength dimensions, Wood et al. proposed surface light field [139]. They first obtained a base mesh of the scene object through a range scanner. For points on the base mesh, they obtained the reflections along different directions by capturing hundreds of images of the scene. A pointwise fairing algorithm was proposed to resample the irregular sample light rays into a reflection map or lumisphere with a piecewise linear model. Notice that these lumispheres may have missing data as only light rays reflected to the outside of the object can be captured. Rendering surface light field is as straightforward as tracing each rendered light ray onto the geometric model and obtain its radiance. A more compact representation of surface light field suitable for an accelerated graphics pipeline was recently proposed in [22]. A surface light field created on the surface of a visual hull rather than the true scene geometry is discussed in [80]. As we mentioned earlier in Section II-A, under Assumption 2 (the radiance of a light ray does not change along its path in empty space), using the visual hull surface for recording the light rays is equivalent to using the true scene geometry as long as the viewpoint is outside the visual hull.

As mentioned before, the surface plenoptic function captures the scene only at a fixed lighting condition. Recently there has been some work on the relighting of IBR, such as the human face reflectance field [26], the plenoptic illumination function [141] and the reflected irradiance field [67]. These approaches share similar ideas. Images of the scene under different point light source or directional light source are first captured. These images can then be superimposed to render scenes under a much more complex lighting environment. Such operation can be performed to live-action scenes in real time [28].

B. Sampling

When certain source description is available, the number of images required is dramatically reduced. Most of the work listed in this section considered the set of reference images as granted and tried to render the scene in the best effort. However, it is still interesting to know how many images we really need for capturing a scene. The problem is in fact much harder than the one discussed in Section II-C for several reasons. First, the sampling rate will certainly be affected by how much source description is known and how good the knowledge is. Second, the rendering

algorithms used in this section are much more difficult to analysis due to the introduction of many assumptions and heuristics. How true these assumptions are will also affect the sampling rate. Last, images used in the IBR representations in this section are usually non-uniformly distributed. Work in [15][149] is not easily extendable to non-uniform sampling analysis.

Uniform sampling with known scene descriptions

We first discuss several approaches that perform uniform sampling with known scene description. In [15], a minimum sampling curve was proposed in the joint image and geometry space for light field. Recall the conclusion in Section II-C that a Lambertian scene at constant depth corresponds to a tilted line in the frequency domain. If the scene geometry is represented via dense depth map and each depth value has a finite precision (a certain number of bits), we may divide the scene into multiple layers based on the depth values. If occlusions between layers are ignored, each layer can be sampled and rendered independently. This is equivalent to having many scenes with much smaller depth variation, which reduces the number of images required. An example minimum sampling curve is shown in Figure 12 (a). Based on this curve, given the number of depth layers, we may tell the minimum number of images needed. On the other hand, given the number of images, we can also tell how many depth layers we need. The minimum sampling curve is also related with the capturing and rendering resolution. The higher the resolution, the more images or depth layers are required, as shown in Figure 12 (b). Such analysis can be easily extended to non-Lambertian and occluded scenes as in [149].
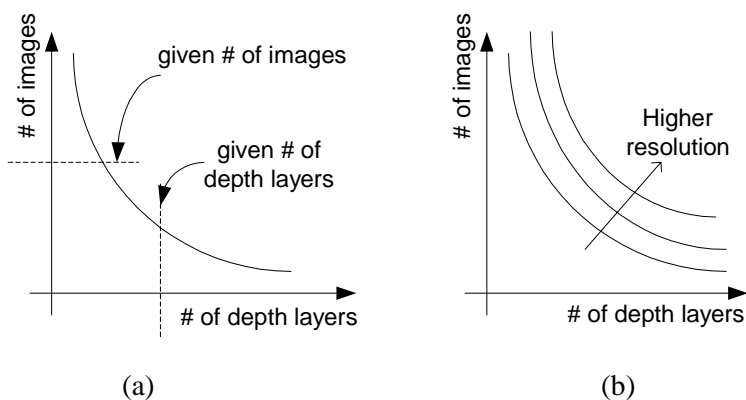

Figure 12 The minimum sampling curve in [15].

Another uniform sampling discussion is on the reflected irradiance field [67]. Reflected irradiance field records the light rays reflected from a scene to a fixed viewpoint as a point light source moves on a plane. It belongs to the category of "IBR with reflection models". The sampling of the positions of the light source is uniform on that plane. To obtain the minimum number of samples required for the light source, they proposed a method based on linear

interpolation and absolute error bound. They concluded that there exists a geometry-independent bound for the sampling interval whenever the second-order derivatives of the surface BRDF and the minimum scene depth are bounded. The fact that such bound is geometry-independent is largely due to the fixed camera position.

Non-uniform sampling

Similar to the eight goals for IBR rendering in [10], Zhang and Chen [151] listed seven desired properties for IBR sampling: adaptive; ease of setup, control and calibration; matching between the viewing space and the capturing space; high and consistent rendering quality; low storage and short capturing time; robust and use robust geometry. Uniform sampling bears some of these properties such as robust and ease of setup, control and calibration, but it lacks most of the other desired properties. On contrary, non-uniform sampling provides a possible solution to all the seven properties.

Note that the sampling approaches discussed below are different from the previously mentioned IBR approaches in this section. Before we focused on how to represent and render a scene given a set of pre-captured images. In uniform sampling analysis we only need to tell how many images are needed. The non-uniform sampling analysis followed need to answer not only how many images are needed but also where to place these cameras.

Fleishman *et al.* [34] proposed an automatic camera placement algorithm for IBR. A mesh model of the scene is known. The goal is to place the cameras optimally such that the captured images can form the best texture map for the mesh model. They found that such problem can be regarded as a 3D art gallery problem, which is NP-hard [97]. They then proposed an approximation solution for the problem by testing a large set of camera positions and selecting the ones with higher gain rank. Here the gain was defined based on the portion of the image that can be used for the texture map. A similar approach was proposed in [136], where the set of reference views were selected from a large image pool in order to minimize a certain target function.

Zhang and Chen proposed to use stochastic sampling and the sampling density function to analyze IBR non-uniform sampling [150]. The idea is to assume that the optimal stochastic sampling strategy on the scene surface is known. Using the Monte Carlo method [43], we may obtain the optimal sampling scheme for the IBR representation. Unfortunately, this approach requires too much knowledge about the scene, such as the scene geometry and the scene surface's optimal sampling density function. The application of such analysis may be limited.

A systematic framework called position-interval-error (PIE) function for studying non-uniform sampling was proposed in [151], using IBR as an example. The PIE function is defined

as the average reconstruction error for any pair of samples, as is shown in Figure 13. Assumptions were made for the PIE function, such as that the average reconstruction error monotonically decreases when the interval between two samples decreases. The goal of non-uniform sampling defined in [151] is to have a uniform reconstruction error across all the sample pairs, which corresponds to one of the desired IBR sampling properties: high and consistent rendering quality.
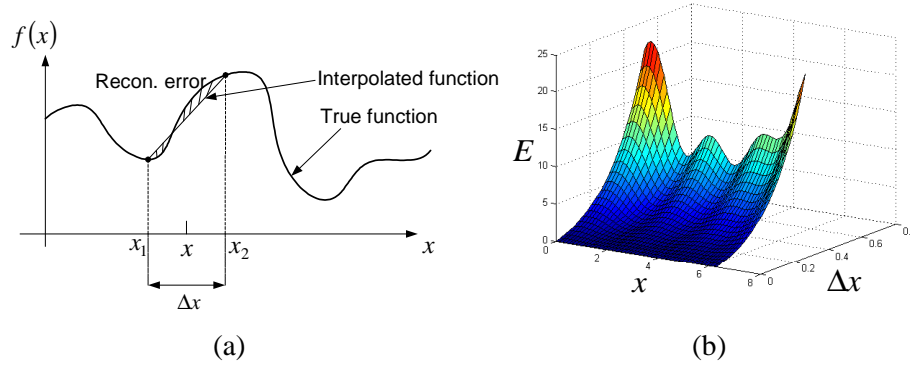

(a)   (b)

Figure 13 An example position-interval-error (PIE) function. (a) The original function, its samples and reconstruction. (b) The PIE function.

Under the PIE framework, two non-uniform sampling approaches were proposed in [151], namely the progressive capturing (PCAP) and the rearranged capturing (RCAP). Both methods adopt an inward-looking concentric mosaics setup, but the samples on the camera trajectory can be non-uniform. To estimate the reconstruction error between two neighboring samples, a simple scheme was proposed based on the color consistency criterion. PCAP is applicable for static scenes. Based on the images captured so far, PCAP determines where to take the next image. The strategy is to always capture the next image between the image pair that has the maximum reconstruction error. RCAP, on the other hand, is for capturing both static and dynamic scenes. The goal is to intelligently arrange the positions of a limited number of cameras such that the final rendering quality is optimal. A force-based method was proposed to move the cameras towards the direction where the reconstruction error is higher. Experimental results demonstrated that the non-uniform sampling approaches outperform the traditional uniform methods.

The PIE framework can also be easily extended to sampling in the high dimensional space. Two previous work, adaptive Lumigraph acquisition [112] and active IBR [147] can both be considered as examples of such extension for PCAP. Again the next image is taken at the place where the reconstruction error is the highest. Slightly different methods were used for estimating the reconstruction error and determining the next capturing positions in the two approaches.

Non-uniform sampling will inevitably increase the complexity of the capturing system in real applications. However building such systems is still possible, such as the simple PCAP system in [146].

C. Compression

The compression of IBR representations with source descriptions in this section has not been widely studied in the literature. However, most of the compression algorithms described in Section II-D can be directly applied for compressing the reference images. On the other hand, there are still the source descriptions needed to be compressed other than the images.

In [53] Krishnamurthy *et al.* considered the compression of depth maps in IBR. Depth map compression is different from traditional image compression because the compression error has different impact on the perceived visual quality. In a depth map, certain regions may be more crucial to the final rendering quality compared to others. For example, they observed that sharp discontinuities in depth and intensity require more accurate depth maps. Accordingly, a region-of-interesting (ROI) based coding scheme was proposed. Also, they found that depth error is more sensitive for closer scene objects and proposed to reshape the dynamic range of the depth image before compression. This observation coincides with the conclusion in [15], which said that the depth quantization should be performed in the disparity space rather than the depth space. A JPEG2000 encoder [127] was used in [53] after the preprocessing.

Duan and Li proposed an algorithm for compressing LDI data [30]. Different from normal image or depth map, in LDI each pixel is associated with multiple colors and depth values. The data were organized layer by layer based on how far the scene is from the viewpoint. One key issue is that for a farther layer, the color and depth map are very sparse. They proposed to aggregate the data first and then perform compression. High compression ratio at about 10:1 to 20:1 was achieved.

For the compression of other geometric models such as mesh models, there have been many approaches in the literature. We refer the reader to [126] for a detailed introduction on geometry compression.

For representations that records the reflected light rays from the scene surface, compression is also desired. In [139], along with the proposed surface light field, Wood *et al.* also proposed two methods to compress the lumispheres, namely function quantization and principal function analysis. Function quantization resembles the traditional vector quantization, and principal function analysis is a generalization to the principle component analysis (PCA). These generalizations are mainly for the purpose of handling the missing data in the lumispheres. In the

light field mapping [22], *Chen et al.* proposed another compression approach that relies on PCA, VQ and S3 texture compression (S3TC^{TM}) [109]. Since real-time rendering was their goal, many decisions made in [22] are due to speed concerns. Compression of the plenoptic illumination function was also discussed in [141] using spherical harmonic transform [24], VQ and DCT.

IV. Conclusions and Future Work

We have surveyed the field of image-based rendering including its representations, sampling and compression. We found that all the IBR representations are originated from the 7D plenoptic function, which describes the appearance of the world. As the 7D plenoptic function has too many data to handle, various approaches were proposed to reduce the data size while still give the viewer a good browsing experience. Two major strategies were adopted: restraining the viewing space and introducing source descriptions. We have presented the various IBR representations based on such categorization. Sampling and compression were discussed separately for the two strategies, as different strategies results in different representations and thus different sampling and compression methods.

It is always exciting to predict some of the future directions for IBR. In terms of representation, IBR through restraining the viewing space is more and more widely adopted in the real world. For example, many websites now provide virtual tour to their place, among which most are based on panoramic images. It is expectable that panoramic videos will be an attractive approach to virtual touring for many resorts. Immersive TV recently receives much attention and is considered as the next generation of TV technology [33]. Other applications include online game, remote education, e-commerce, virtual museum, virtual reality/chat room, etc. The key to the success of IBR representations through restraining the viewing space in the future is the relaxation of these constraints. We may count on the rapid increasing of storage and memory space, as well as the increasing of the Internet bandwidth. More devices may need to be developed (such as dense camera array) in order to capture large, dynamic scenes.

IBR through introducing source descriptions, on the other hand, still requires more future work. The key problem is not how to perform the rendering, but how to obtain a good source description. Take the scene geometry as an example. There have been many geometry reconstruction algorithms proposed in the computer vision literature. However, few of them are really robust enough to be applied in practical systems. To solve this problem, either we may develop some low-cost 3D sensing devices, or we may develop new algorithms that can perform good source description reconstruction.

The rendering process in IBR is usually very fast and can be implemented with software. However, hardware acceleration will be definitely helpful for future high-resolution IBR rendering. As most operations in IBR rendering are simple mathematical operations such as linear interpolation, and most IBR rendering process can be performed in parallel, we expect that such hardware is not difficult to develop and can dramatically increase the rendering speed.

No matter how much the storage and memory increase in the future, sampling and compression are always useful to keep the IBR data at a manageable size. The work on sampling and compression, however, has just started. There are still many problems remain unsolved, such as the sampling rate when certain source description is available. A high compression ratio in IBR seems rely heavily on how good the images can be predicted, which depends on, e.g., how good a certain source description can be reconstructed. Joint work between the signal processing community and the computer vision community is highly expected.

Image-based rendering is still an emerging field. From this survey, it is obvious that IBR has attracted many researchers from various communities, including computer graphics, computer vision and signal processing. We believe that the cooperation of different communities will certainly bring a bright future for IBR.

Reference

[1]   360 One VR^{TM}, Kaidan, http://www.kaidan.com/.

[2]   E. H. Adelson, and J. R. Bergen, "The plenoptic function and the elements of early vision", *Computational Models of Visual Processing*, Edited by Michael Landy and J. Anthony Movshon. The MIT Press, Cambridge, Mass. 1991, Chapter 1.

[3]   G. Agarwal, D. Rathi, P. K. Kalra and S. Banerjee, "A System for Image Based Rendering of Walk-throughs", *Computer Graphics International (CGI2002)*, Bradford, UK, July 2002.

[4]   T. Akenine-Moller and E. Haines, *Real-Time Rendering*, 2nd Edition, A K Peters Ltd.

[5]   D. G. Aliaga and I. Carlbom, "Plenoptic stitching: a scalable method for reconstructing 3D interactive walkthroughs", *Computer Graphics (SIGGRAPH'01)*, August 2001, pp. 443-450.

[6]   S. Avidan and A. Shashua, "Novel view synthesis in tensor space", *CVPR'97*, San Juan, Puerto Rico, 1997, pp. 1034-1040.

[7]   T. Beier and S. Neely, "Feature-Based Image Metamorphosis", *Computer Graphics (SIGGRAPH'92)*, July 1992, pp. 35-42.

[8]   J. F. Blinn and M. E. Newell, "Texture and Reflection in Computer Generated Images", *Communications of the ACM*, Vol. 19, No. 10, 1976, pp. 542-546.

[9]   S. Borman and R. L. Stevenson, "Super-Resolution from Image Sequences - A Review", *Midwest Symposium on Circuits and Systems*, 1998.

[10]   C. Buehler, M. Bosse, L. McMillan, S. Gortler, and M. Cohen,   "Unstructured Lumigraph rendering", *Computer Graphics (SIG-GRAPH'01)*, August 2001, pp 425-432.

[11]   CBS Broadcasting Inc., http://www.cbs.com.

[12]   B. Cabral, M. Olano, P. Nemec, "Reflection space image based rendering", *Computer Graphics (SIGGRAPH'99)*, August 1999, pp. 165-171.

[13]   E. Camahort and D. Fussell, "A Geometric Study of Light Field Representations", *Technical Report TR99-35*, Department of Computer Sciences, The University of Texas at Austin.

[14]   E. Camahort, A. Lerios and D. Fussell, "Uniformly sampled light fields", *9th Eurographics Workshop on Rendering*, Vienna, Austria, June/July 1998, pp. 117-130.

[15]   J.X. Chai, X. Tong, S.C. Chan and H. Y. Shum, "Plenoptic sampling", *Computer Graphics (SIGGRAPH'00)*, July 2000, pp. 307-318.

[16]   S. C. Chan, K. T. Ng, Z. F. Gan, K. L. Chan and H.-Y. Shum, "The Data Compression of Simplified Dynamic Light Fields", *ICASSP'03*, Hong Kong, Apr. 2003.

[17]   S. C. Chan and H. Y. Shum, "A Spectral Analysis for Light Field Rendering", *ICIP'00*, Vancouver, Canada, Sep. 2000.

[18]   C. Chang, G. Bishop and A. Lastra, "LDI tree: A hierarchical representation for image-based rendering", *Computer Graphics (SIGGRAPH'99)*, August 1999, pp. 291-298.

[19]   C.-L. Chang, X. Zhu, P. Ramanathan and B. Girod, "Shape Adaptation for Light Field Compression", *ICIP'03*, Barcelona, Spain, Sep. 2003.

[20]   S. E. Chen, "QuickTime VR – An Image-Based Approach to Virtual Environment Navigation", *Computer Graphics (SIGGRAPH'95)*, August 1995, pp. 29-38.

[21]   S. E. Chen and L. Williams, "View interpolation for image synthesis", *Computer Graphics (SIGGRAPH'93)*, August 1993, pp. 279-288.

[22]   W.-C. Chen, J.-Y. Bouguet, M. H. Chu, R. Grzeszczuk, "Light field mapping: efficient representation and hardware rendering of surface light fields", *Computer Graphics (SIGGRAPH'02)*, July 2002, pp. 447-456.

[23]   T. N. Cornsweet, *Visual Perception*, Academic Press, 1971.

[24]   R. Courant and D. Hilbert, *Methods of Mathematical Physics*, New York: Interscience, 1953.

[25]   P. Debevec, "Rendering Synthetic Objects into Real Scenes: Bridging Traditional and Image-Based Graphics with Global Illumination and High Dynamic Range Photography", *Computer Graphics (SIGGRAPH'98)*, Aug. 1998, pp. 189-198.

[26]   P. Debevec, T. Hawkins, C. Tchou, H.-P. Duiker, W. Sarokin and M. Sagar, "Acquiring the Reflectance Field of a Human Face", *Computer Graphics (SIGGRAPH'00)*, July 2000, pp. 145-156.

[27]   P. Debevec, C. J. Taylor and J. Malik, "Modeling and rendering architecture from photographs: a hybrid geometry- and image-based approach", *Computer Graphics (SIGGRAPH'96)*, August 1996, pp. 11-20.

[28]   P. Debevec, A. Wenger, C. Tchou, A. Gardner, J. Waese and T. Hawkins, "A Lighting Reproduction Approach to Live-Action Compositing", *Computer Graphics (SIGGRAPH'02)*, July 2002, pp. 547-556.

[29]   P. Debevec, Y.-Z. Yu and G. Borshukov, "Efficient View-Dependent Image-Based Rendering with Projective Texture-Mapping", *9th Eurographics Rendering Workshop*, Vienna, Austria, June 1998.

[30]   J. G. Duan and J. Li, "Compression of the Layered Depth Image", *IEEE Data Compression Conference (DCC'01)*, Snowbird, UT, Mar. 2001.

[31]   D. E. Dudgeon and R.M. Mersereau, *Multidimensional Digital Dignal Processing*, Prentice-hall signal processing series, 1984.

[32]   P. Eisert, E. Steinbach and B. Girod, "3-D Shape Reconstruction from Light Fields Using Voxel Back-Projection", *Vision, Modeling and Visualization Workshop 1999*, Erlangen, Germany, November, 1999, pp. 67-74.

[33]   C. Fehn, P. Kauff, O. Schreer and R. Schäfer, "Interactive Virtual View Video for Immersive TV Applications", *Proc. IBC '01*, Vol. 2, Amsterdam, Netherlands, Sep. 2001, pp. 53-62.

[34]   S. Fleishman and D. Cohen-Or and D. Lischinski, "Automatic Camera Placement for Image-Based Modeling", *Computer Graphics Forum*, Vol. 19, No. 2, Jun. 2000.

[35]   J. Foote and D. Kimber, "FlyCam: Practical Panoramic Video", *Proc. ICME'00*, August 2000.

[36]   B. Girod, C.-L. Chang, P. Ramanathan and Xiaoqing Zhu, "Light field compression using disparity-compensated lifting", *ICASSP'03*, Hong Kong, China, Apr. 2003.

[37]   S. J. Gortler, R. Grzeszczuk, R. Szeliski and M. F. Cohen, "The Lumigraph", *Computer Graphics (SIGGRAPH'96)*, August 1996, pp. 43-54.

[38]   N. Greene and P. Heckbert, "Creating Raster Omnimax Images from Multiple Perspective Views Using the Elliptical Weighted Average Filter", *IEEE Computer Graphics and Applications*, pp. 21-27, Vol. 6, No. 6, June 1986.

[39]   N. Greene and M. Kass, "Approximating Visibility with Environment Maps", *Technical Report #41*, Apple Computer, November 1994.

[40]   C. Grünheit, A. Smolić, and T. Wiegand, "Efficient representation and interactive streaming of high-resolution panoramic views", *ICIP'02*, Rochester, NY, Sep. 2002.

[41]   X. Gu, S. J. Gortler and M. Cohen, "Polyhedral Geometry and the Two-Plane Parameterization", *8th Eurographics Rendering Workshop*, Saint Etienne, France, June 1997, pp. 1-12.

[42]   R. Gupta, R. I. Hartley, "Linear pushbroom cameras", *IEEE Trans. on PAMI*, Vol. 19 No. 9, Sep. 1997, pp. 963-975.

[43]   J. H. Halton, "A Retrospective and Prospective Survey of the Monte Carlo Method", *SIAM Review*, Vol. 12, No. 1, Jan. 1970, pp. 1-63.

[44]   R. Hartley, A. Zisserman, *Multiple View Geometry in Computer Vision*, Cambridge University Press, Sep. 2000.

[45]   I. Ihm, S. Park, and R. Lee, "Rendering of spherical light fields", *Pacific Graphics*, Seoul, Korea, October 1997, pp. 59-68.

[46] IPIX®, Internet Pictures Corp., http://www.ipix.com/.

[47] A. Isaksen, L. McMillan, S. J. Gortler, "Dynamically reparameterized light fields", *Computer Graphics (SIGGRAPH'00)*, July 2000, pp. 297-306.

[48] S. B. Kang, "A survey of image-based rendering techniques", *VideoMetrics*, SPIE Vol. 3641, 1999, pp. 2-16.

[49] S.B. Kang, R. Szeliski, and P. Anandan, "The geometry-image representation tradeoff for rendering," *ICIP'00*, Vancouver, Canada, September 2000.

[50] A. Katayama, K. Tanaka, T. Oshino and H. Tamura, "Viewpoint-dependent stereoscopic display using interpolation of multi-viewpoint images", *Proc. SPIE*, Vol.2409, 1995, pp.11-20.

[51] H. Kawasaki, K. Ikeuchi and M Sakauchi, "Light field rendering for large-scale scenes ", *Proc. CVPR'01*, Kauai, Hawaii, Dec. 2001, Vol.2, pp.64-71.

[52] D. Kimber, J. Foote and S. Lertsithichai, "FlyAbout: Spatially Indexed Panoramic Video", *Proc. ACM Multimedia 2001*, Ottawa, Canada, Oct. 2001.

[53] R. Krishnamurthy, B.-B. Chai, H. Tao and S. Sethuraman, "Compression and Transmission of Depth Maps for Image-Based Rendering", *ICIP'01*, Thessaloniki, Greece, Oct. 2001.

[54] Ladybug^TM, Point Grey, http://www.ptgrey.com/products/ladybug/index.html.

[55] P. Lalonde and A. Fournier, "Interactive Rendering of Wavelet Projected Light Fields", *Graphics Interface 1999*, Kingston, Ontario, Canada, Sep. 1999, p.107-114.

[56] S. Laveau and O. Faugeras, "3-D Scene Representation as a Collection of Images and Fundamental Matrices", *Technical Report 2205*, INRIA, Feb. 1994.

[57] A. Laurentini, "The Visual Hull Concept for Silhouette Based Image Understanding." *IEEE PAMI*, Vol. 16, No. 2, 1994, pp. 150-162.

[58] S. Lee, K.-Y. Chwa, J. Hahn and S.Y. Shin, "Image Morphing Using Deformation Techniques", *Journal of Visualization and Computer Animation*, Vol. 7, No. 1, 1996, pp. 3-23.

[59] J. Lengyel, "The convergence of graphics and vision", *Technical Report, IEEE Computer*, July 1998.

[60] H. Lensch, "Techniques for Hardware-Accelerated Light Field Rendering", *Master Thesis*, Friedrich-Alexander-Universität Erlangen-Nürnberg, 1999.

[61] W. H. Leung and T. Chen, "Line-Space Representation and Compression for Image-Based Rendering", *Carnegie Mellon Technical Report: AMP01-02*.

[62] M. Levoy and P. Hanrahan, "Light field rendering", *Computer Graphics (SIGGRAPH'96)*, August 1996, pp. 31-42.

[63] M. Lhuillier and L. Quan, "Image Interpolation by Joint View Triangulation", *Proc. CVPR'99*, Fort Collins, USA, June 1999.

[64] J. Li, H. Shum and Y. Zhang, "On the compression of the image based rendering scene: a comparison among block, reference and wavelet coders", *International Journal on Image and Graphics*, Vol. 1, No. 1, 2001, pp.45-61.

[65] J. Li, K. Zhou, Y. Wang and H.-Y. Shum, "A Novel Image-Based Rendering System With A Longitudinally Aligned Camera Array", *EUROGRAPHICS'00*, Interlaken, Switzerland, Aug. 2000, pp.107-114.

[66] Z. C. Lin and H. Y. Shum, "On the Number of Samples Needed in Light Field Rendering with Constant-Depth Assumption", *Proc. CVPR'00*, Hilton Head Island, South Carolina, USA, June 2000.

[67] Z.-C. Lin, T.-T. Wong and H.-Y. Shum, "Relighting with the Reflected Irradiance Field: Representation, Sampling and Reconstruction", *International Journal of Computer Vision*, Vol. 49, No. 2-3, Sep.-Oct. 2002, pp. 229-246.

[68] A. Lippman, "Movie Maps: An Application of the Optical Videodisc to Computer Graphics", *Computer Graphics (Proc. SIGGRAPH'80)*, 1980, pp. 32-43.

[69] D. Lischinski and A. Rappoport, "Image-Based Rendering for Non-Diffuse Synthetic Scenes", *Rendering Techniques '98*, Vienna, Austria, June 1998.

[70] W. Lorensen and H. Cline, "Marching Cubes: A High Resolution 3-D Surface Construction Algorithm", *Computer Graphics (SIGGRAPH'87)*, Anaheim, CA, July 1987, pp. 163-169.

[71] L. Luo, Y. Wu, J. Li, and Y. Zhang, "Compression of concentric mosaic scenery with alignment and 3D wavelet transform", *SPIE: Image and Video Commun. And Processing 2000*, San Jose CA, January 2000, pp. 89-100.

[72] M. Magnor, P. Eisert, B. Girod, "Model-Aided Coding of Multi-Viewpoint Image Data", *ICIP'00*, Vancouver, Canada, 2000, pp. 919-922.

[73] M. Magnor and B. Girod, "Adaptive Block-Based Light Field Coding", *3rd Int. Workshop on Synthetic and Natural Hybrid Coding and Three-Dimensional Imaging (IWSNHC3DI'99)*, Santorini, Greece, Sep. 1999.

[74] M. Magnor and B. Girod, "Hierarchical Coding of Light Fields with Disparity Maps", *ICIP'99*, Kobe, Japan, Oct. 1999.

[75] M. Magnor and B. Girod, "Data compression for light field rendering", *IEEE Trans. on CSVT*, Vol. 10, No. 3, Apr. 2000, pp. 338-343.

[76] M. Magnor and B. Girod, "Model-Based Coding of Multi-Viewpoint Imagery", *VCIP'00*, Perth, Australia, June 2000.

[77] D. Marchand-Maillet and M. Vetterli, "Sampling Theory for Image-Based Rendering", *Master thesis*, EPFL, Apr. 2001.

[78] W. R. Mark, L. McMillan and G. Bishop, "Post-rendering 3D warping", *Proc. 1997 Symposium on Interactive 3D Graphics*, ACM Press, 1997, pp. 7-16.

[79] W. Matusik, C. Buehler, R. Raskar, S. Gortler, and L. McMillan, "Image-based Visual Hulls", *Computer Graphics (SIGGRAPH'00)*, July 2000, pp. 369-374.

[80] W. Matusik, H. Pfister, A. Ngan, P. Beardsley, R. Ziegler and L. McMillan, "Image-based 3D photography using opacity hulls", *Computer Graphics (SIGGRAPH'02)*, July 2002, pp. 427-437.

[81]   L. McMillan, "An Image-Based Approach to Three-Dimensional Computer Graphics", *Ph.D. Thesis*, Department of Computer Science, University of North Carolina at Chapel Hill, 1997.

[82]   L. McMillan and G. Bishop, "Plenoptic modeling: an image-based rendering system", *Computer Graphics (SIGGRAPH'95)*, August 1995, pp. 39-46.

[83]   J. Meehan, *Panoramic Photograph*, Watson-Guptill, 1990.

[84]   D.L. Milgram, "Computer methods for creating photomosaics", *IEEE Trans. Comput.* C-24, 1975, pp. 1113-1119.

[85]   G. Miller, E. Hoffert, S. E. Chen, E. Patterson, D. Blackketter, S. Rubin, S. A. Aplin, D. Yim, J. Hanan, "The Virtual Museum: Interactive 3D Navigation of a Multimedia Database", *The Journal of Visualization and Computer Animation*, Vol. 3, No. 3, 1992, pp. 183-197.

[86]   G. Miller, S. Rubin, and D. Ponceleon, "Lazy decompression of surface light fields for precomputed global illumination", *Eurographics Rendering Workshop 1998*, Vienna, Austria, June 1998, pp. 281-292.

[87]   J. L. Mitchell, W. B. Pennebaker, C. E. Fogg, and D. J. LeGall, *MPEG video: compression standard*, Chapman & Hall, 1996.

[88]   S. Nayar, "Catadioptric omnidirectional camera", *Proc. CVPR'97*, Puerto Rico, June 1997, pp. 482-488.

[89]   U. Neumann, T. Pintaric, A. Rizzo, "Immersive Panoramic Video", *Proc. ACM Multimedia 2000*, October 2000, pp. 493-494.

[90]   K. T. Ng, S. C. Chan and H.-Y. Shum, "Scalable Coding and Progressive Transmission of Concentric Mosaic Using Nonlinear Filter Banks", *ICIP'01*, Thessaloniki, Greece, Oct. 2001.

[91]   K. T. Ng, S. C. Chan, H.-Y. Shum and S. B. Kang, "On the Data Compression and Transmission Aspects of Panoramic Video", *ICIP'01*, Thessaloniki, Greece, Oct. 2001.

[92]   T. Nishita, T. Fujii and E. Nakamae, "Metamorphosis Using Bézier Clipping", *Proc. of the First Pacific Conference on Computer Graphics and Applications*, Seoul, Korea, 1993.

[93]   J. R. Ohm, "Three-dimensional subband coding with motion compensation", *IEEE Trans. on Image Processing*, Vol. 3, No. 5, Sep. 1994, pp. 559-571.

[94]   M. Oliveira, "Image-Based Modeling and Rendering Techniques: A Survey", *RITA - Revista de Informática Teórica e Aplicada*, Volume IX, Number 2, October 2002, pp. 37-66.

[95]   M. Oliveira and G. Bishop, "Relief textures", *Technical report, UNC Computer Science TR99-015*, March 1999.

[96]   A. V. Oppenheim, A. S. Willsky, S. N. Nawab, S. H. Nawab, H. Nawad, S. H. Nawab, *Signals and Systems*, 2nd Edition, Prentice Hall, 1996.

[97]   J. O'Rourke, *Art Gallery Theorems and Algorithms*, The International Series of Monographs on Computer Science. Oxford University Press, New York, NY, 1987.

[98]   V. Padmanabhan and J. Mogul, "Using Predictive Prefetching to Improve World-Wide Web Latency", *Proc. SIGCOMM'96*, Stanford University, California, Aug. 1996.

[99] S. Peleg and M. Ben-Ezra, "Stereo Panorama with a Single Camera", *Proc. CVPR'99*, Ft. Collins, Colorado, June 1999.

[100] S. Peleg and J. Herman, "Panoramic Mosaics by Manifold Projection", *Proc. CVPR'97*, Washington, June 1997, pp. 338-343.

[101] S. Peleg, B. Rousso, A. Rav-Acha, A. Zomet, "Mosaicing on adaptive manifolds", *IEEE Trans. on PAMI*, Vol. 22 No. 10, Oct 2000, pp. 1144-1154.

[102] T. Ebrahimi and F. Pereira, *The MPEG-4 Book*, Prentice Hall PTR, July 2002.

[103] I. Peter and W. Straßer, "The Wavelet Stream - Progressive Transmission of Compressed Light Field Data", *IEEE Visualization 1999*, San Francisco, CA.

[104] P. Rademacher, "View-dependent geometry", *Computer Graphics (SIGGRAPH'99)*, August 1999, pp. 439-446.

[105] P. Rademacher and G. Bishop, "Multiple-center-of-projection images", *Computer Graphics (SIGGRAPH'98)*, August 1998, pp. 199-206.

[106] P. Ramanathan, M. Kalman and B. Girod, "Rate-Distortion Optimized Streaming of Compressed Light Fields", *ICIP'03*, Barcelona, Spain, Sep. 2003.

[107] P. Ramanathan, E. Steinbach, P. Eisert and B. Girod, "Geometry refinement for light field compression", *ICIP'02*, Rochester, NY, Sep. 2002.

[108] D. G. Ripley, "DVI-a Digital Multimedia Technology", *Communications of the ACM*, Vol. 32 No. 7, 1989, pp. 811-822.

[109] S3TC^TM, SONICblue Incorporated, http://www.s3.com/.

[110] H. S. Sawhney and R. Kumar, "True multi-image alignment and its application to mosaicing and lens distortion correction", *IEEE Trans. PAMI*, Vol. 21 No. 3, Mar. 1999, pp. 235-243.

[111] D. Scharstein and R. Szeliski, "A Taxonomy and Evaluation of Dense Two-Frame Stereo Correspondence Algorithms", *Int. Journal of Computer Vision*, Vol. 47, No. 1/2/3, Apr.-Jun. 2002, pp7-42.

[112] H. Schirmacher, W. Heidrich and H. P. Seidel, "Adaptive Acquisition of Lumigraphs from Synthetic Scenes", *EUROGRAPHICS'99*, Vol. 18, No. 3, 1999.

[113] H. Schirmacher, W. Heidrich and H. P. Seidel. "High-quality interactive Lumigraph rendering through warping" *Graphics Interface 2000*, Montreal, Canada, May 2000.

[114] I. O. Sebe, P. Ramanathan and B. Girod, "Multi-View Geometry Estimation for Light Field Compression", *Proc. Vision, Modeling and Visualization (VMV-2002)*, Erlangen, Germany, Nov. 2002, pp. 265-272.

[115] S. M. Seitz and C. R. Dyer, "Photorealistic Scene Reconstruction by Voxel Coloring", *Proc. CVPR'97*, San Juan, Puerto Rico, June 1997, pp. 1067-1073.

[116] S. M. Seitz and C. R. Dyer, "Physically-Valid View Synthesis by Image Interpolation", *Proc. Workshop on Representation of Visual Scenes*, 1995, pp. 18-25.

[117] S. M. Seitz and C. M. Dyer, "View morphing", *Computer Graphics (SIGGRAPH'96)*, August 1996, pp. 21-30.

[118] J. Shade, S. Gortler, L.-W. He and R. Szeliski, "Layered depth images", *Computer Graphics (SIGGRAPH'98)*, August 1998, pp. 231-242.

[119] H.-Y. Shum and L.-W. He, "Rendering with concentric mosaics", *Computer Graphics (SIGGRAPH'99)*, August 1999, pp.299-306.

[120] H.-Y. Shum, K. T. Ng and S. C. Chan, "Virtual Reality Using the Concentric Mosaic: Construction, Rendering and Data Compression", *ICIP'00*, Vancouver, Canada, Sep. 2000, pp. 644-647.

[121] H.-Y. Shum, L.-F. Wang, J.-X. Chai and X. Tong, "Rendering with Manifold Hopping", *International Journal of Computer Vision*, Vol. 50, No. 2, Nov. 2002, pp. 185-201.

[122] P. P. Sloan, M. F. Cohen and S. J. Gortler, "Time critical Lumigraph rendering", *Symposium on Interactive 3D Graphics*, Providence, RI, USA, 1997, pp.17-23.

[123] R. Swaminathan and S.K. Nayar, "Polycameras: Camera Clusters for Wide Angle Imaging", *Columbia University Technical Report, CUCS-013-99*.

[124] R. Szeliski, "Image Mosaicing for Tele-Reality Applications", *Technical Report CRL94/2*, DEC Cambridge Research Lab, May 1994.

[125] R. Szeliski and H.-Y. Shum, "Creating full view panoramic image mosaics and texture-mapped models", *Computer Graphics (SIGGRAPH'97)*, August 1997, pp. 251-258.

[126] G. Taubin and J. Rossignac, *Course 38: 3D Geometry Compression, Siggraph'2000 Course Notes*, July 2000.

[127] D. Taubman and M. Marcellin, *Jpeg2000: Image Compression Fundamentals, Standards, and Practice*, Kluwer Academic Publishers, Nov. 2001.

[128] D. Taubman and A. Zakhor, "Multirate 3-D subband coding of video", *IEEE Trans. on Image Processing*, Vol. 3, No. 5, Sep. 1994, pp. 572-588.

[129] S. Teller, M. Antone, Z. Bodnar, M. Bosse, S. Coorg, M. Jethwa, N. Master, "Calibrated, Registered Images of and Extended Urban Area", to appear in the *International Journal of Computer Vision*, 2003.

[130] J. Y. Tham, S. Ranganath, and A. A. Kassim, "Highly scalable wavelet-based video codec for very low bit-rate environment", *IEEE Journal on Selected Areas in Communications*, vol. 16, no. 1, Jan. 1998.

[131] X. Tong and R. M. Gray, "Coding of Multi-View Images for Immersive Viewing", *ICASSP'00*, Istanbul, Turkey, vol. 4, June 2000, pp. 1879-1882.

[132] TotalView[TM], Be Here Technologies, http://www.behere.com/.

[133] M. Uyttendaele A. Eden, R. Szeliski, "Eliminating Ghosting and Exposure Artifacts in Image Mosaics", *Proc. CVPR'01*, Kauai, Hawaii, Dec. 2001, pp. 509-516.

[134] S. Vedula, S. Baker and T. Kanade, "Spatio-Temporal View Interpolation", *Proc. of the 13th ACM Eurographics Workshop on Rendering*, June, 2002.

[135] T. Werner, R. D. Hersch and V. Hlavác, "Rendering Real-World Objects Using View Interpolation", *Proc. ICCV'95*, Boston, MA, June 1995.

[136] T. Werner, V. Hlavác, A. Leonardis and T. Pajdla, "Selection of Reference Views for Image-Based Representation", *Proc. ICPR'96*, Vienna, Austria, Aug. 1996, pp.73-77.

[137] B. Wilburn, M. Smulski, H.-H. K. Lee and M. Horowitz, "The Light Field Video Camera", *Proceedings of Media Processors 2002, SPIE Electronic Imaging 2002*.

[138] G. Wolberg, *Digital Image Warping*, IEEE Computer Society Press, 1990.

[139] D. N. Wood, D. I. Azuma, K. Aldinger, B. Curless, T. Duchamp, D. H. Salesin and W. Stuetzle, "Surface light fields for 3D photography", *Computer Graphics (SIGGRAPH'00)*, July 2000, pp. 287-296.

[140] D. N. Wood, A. Finkelstein, J. F. Hughes, C. E. Thayer and D. H. Salesin, "Multiperspective panoramas for cel animation", *Computer Graphics (SIGGRAPH'97)*, August 1997, pp.243-250.

[141] T.-T. Wong, C. W. Fu, P.-A. Heng and C.-S. Leung, "The Plenoptic Illumination Function", *IEEE Trans. on Multimedia*, Vol. 4, No. 3, Sep. 2002, pp. 361-371.

[142] Y. Wu, L. Luo, J. Li and Y. Zhang, "Rendering of 3D Wavelet Compressed Concentric Mosaic Scenery with Progressive Inverse Wavelet Synthesis (PIWS)", *VCIP'00*, Perth, Australia, June 2000.

[143] Y. Wu, C. Zhang and J. Li, "Smart-Rebinning for Compression of Concentric Mosaic", *IEEE Trans. on Multimedia*, Vol. 4, No. 3, Sep. 2002, pp 332-342.

[144] Y. Xiong and K. Turkowski, "Creating image-based VR using a self-calibration fisheye lens", *Proc. CVPR'97*, Puerto Rico, June 1997, pp. 237-243.

[145] J. C. Yang, M. Everett, C. Buehler and L. McMillan, "A Real-Time Distributed Light Field Camera", *Eurographics Workshop on Rendering 2002*, pp. 1-10.

[146] C. Zhang and T. Chen, "A System for Active Image-Based Rendering", *ICME'03*, Baltimore, Maryland, July 2003.

[147] C. Zhang and T. Chen, "Active Scene Capturing for Image-Based Rendering", *Carnegie Mellon Technical Report: AMP03-02*.

[148] C. Zhang and T. Chen, "Generalized Plenoptic Sampling", *Carnegie Mellon Technical Report: AMP01-06*.

[149] C. Zhang and T. Chen, "Spectral Analysis for Sampling Image-Based Rendering Data", to appear in *IEEE Trans. on CSVT, Special Issue on Image-based Modeling, Rendering and Animation*.

[150] C. Zhang and T. Chen, "Surface Plenoptic Function as a Tool for Image-Based Rendering Sampling Analysis", *ICASSP'03*, Hong Kong, China, April 2003.

[151] C. Zhang and T. Chen, "Non-Uniform Sampling of Image-Based Rendering Data with the Position-Interval-Error (PIE) Function", *VCIP'03*, Lugano, Switzerland, July 2003.

[152] C. Zhang and J. Li, "Compression of Lumigraph with Multiple Reference Frame (MRF) Prediction and Just-In-Time Rendering," *Proc. IEEE Data Compression Conf. (DCC'00)*, Snowbird, Utah, March 2000, pp. 254-263.

[153] C. Zhang and J. Li, "Compression and Rendering of Concentric Mosaics with Reference Block Codec (RBC)", *VCIP'00*, Perth, Australia, June 2000.

[154] C. Zhang and J. Li, "Interactive Browsing of 3D Environment over the Internet", *VCIP'01*, San Jose, CA, Jan. 2001.

[155] Z.-P. Zhang, L.-F. Wang, B.-N. Guo, H.-Y. Shum, "Feature-based light field morphing", *Computer Graphics (SIGGRAPH'02)*, July 2002, pp. 457-464.

[156] Z.-Y. Zhang, "Image-based geometrically-correct photorealistic scene / object modeling (IBPhM): a review", *Asian Conference on Computer Vision (ACCV'98)*, Hong Kong, Jan. 8-11, 1998.

[157] J. Y. Zheng and S. Tsuji, "Panoramic Representation of Scenes for Route Understanding", *Proc. ICPR'90*, June 1990, pp. 161-167.